PERGAMON

Journal of Asian Earth Sciences 18 (2000) 47–69

Journal of Asian Earth Sciences

Thermal history of Australian passive margin cover sequences accreted to Timor during Late Neogene arc–continent collision, Indonesia

Ron Harris[a,*], James Kaiser[b], Anthony Hurford[c], Andy Carter[c]

[a]*Department of Geology, Brigham Young University, Provo, UT, USA*
[b]*Exxon, Houston, TX, USA*
[c]*Department of Geological Sciences, University College, London, UK*

Received 6 November 1998; accepted 30 April 1999

Abstract

Paleotemperature indicators and apatite fission track analysis of Australian continental margin cover sequences accreted to the active Banda arc–continent collision indicate little to no heating during rapid late Neogene uplift and exhumation. Thermal maturation patterns of vitrinite reflectance, conodont alteration and illite crystallinity show that peak paleotemperatures (PPT) increase with stratigraphic and structural burial. The highest PPT is found in the northern hinterland of the accretionary wedge, which was beneath progressively thicker parts of the upper plate towards the north. Major discontinuities in the pattern of PPT are associated with the position of major thrust ramps such as those forming the Ramelau/Kekneno Arch (RKA). PPT for Upper Triassic to Neogene strata south of the RKA are 60–80°C, which are similar to, and in many cases lower than, correlative and age equivalent units drilled on the NW Australian Shelf. Permian to Lower Triassic sedimentary strata thrust over younger units within and north of the RKA have PPT of 100–220°C. Thrust sheets accreted beneath the upper plate have PPT approximately 90°C higher than those frontally accreted. Metamorphism of the northernmost units of these sequences yield PPT of >300°C. Thrust stacking yields an inverted thermal profile of PPT decreasing discontinuously downward and to the south (towards the foreland). The timing of PPT is constrained by apatite fission track ages from mostly Triassic continental margin cover sequences. Ages of Upper Triassic units are primarily coeval with deposition and show little evidence of thermal annealing, whereas those of Lower Triassic units are almost completely annealed and range from 1.8 ± 0.5–19.2 ± 9.7 Ma. The clustering of apatite fission track ages into two distinct groups indicates that the upper boundary of the partial annealing zone has remained for some time at a Triassic stratigraphic interval in the slope and rise of the NW Australian continental margin. The position of this zone on the present shelf is higher in the stratigraphic column due to the greater thickness of post-breakup shelf facies units. Thrust stacking of rise, slope and shelf units produces an inverted vertical profile of increasing apatite fission track age with depth. Lack of any long confined track lengths in apatite from all of the units requires rapid and recent exhumation of the thrust stack, which is coincident with rapid phases of Pliocene–Pleistocene exhumation documented throughout Timor. These data preclude pre-Late Miocene tectonic burial or pre-Pliocene exhumation of the NW Australian continental margin.

1. Introduction

Sedimentary cover sequences of the NW continental margin of Australia accumulated in intracratonic basins that formed during Permian to Jurassic extension, which gave way to Late Jurassic sea floor spreading and passive margin development (e.g. Falvey, 1972; Veevers et al., 1974; Larson, 1975; Veevers and Cotterill, 1976; Powell, 1976). Sedimentary accumulation continued on the passive margin until Miocene collision with the Java Trench (Carter et al., 1976; Hamilton, 1979; Bowin et al., 1980; von Rad and

* Corresponding author.
E-mail address: rharris@byu.edu (R. Harris).

1367-9120/00/$ - see front matter
PII: S1367-9120(99)00036-X

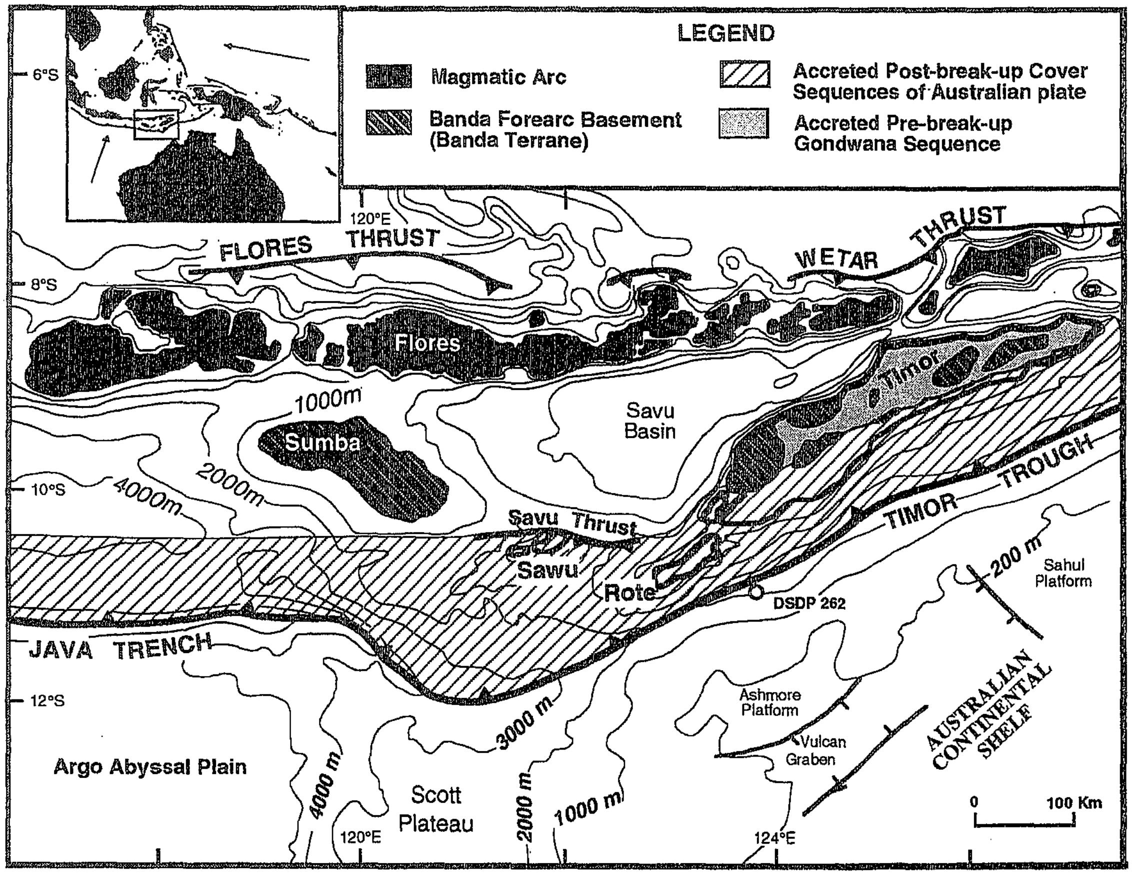

Fig. 1. Simplified tectonic map of the western Banda arc orogen and NW Australian continental margin (see inset for location map and plate convergence vectors). The Java Trench and Timor Trough separate the NNE moving Australian Plate to the south from the Asian Plate to the north. Indian oceanic lithosphere subducts beneath the Java Trench and carries Australian continental lithosphere into the Timor Trough. Australian Plate material accreted to the Asian Plate is shown in stripes (frontal accretionary wedge of post-breakup sedimentary cover sequences) and shading (subcretionary pre-breakup continental cover sequences). Accreted units of the Australian Plate are structurally stacked beneath and in front of parts of the Banda forearc (Banda Terrane, dark stripes). Tectonic boundaries are modified from Hamilton (1979) and Breen et al. (1986).

Exon, 1983; Audley-Charles, 1983). This contractional event has thrust sedimentary cover sequences of the continental rise and slope up onto the NW Australian Shelf along with fragments of the Banda forearc. The thrust stack forms the bulk of the outer Banda arc islands of Eastern Indonesia (Fig. 1). Studies of these rocks provide many important constraints for reconstructing the sedimentary and structural evolution of the northern Australian continental margin and Banda Arc orogenic wedge (Barber and Audley-Charles, 1976; Carter et al., 1976; Barber, 1981; Berry and Grady, 1981; Audley-Charles, 1983, 1988; Audley-Charles and Harris, 1990; Bird and Cook, 1991; Harris, 1991; Sawyer et al., 1993).

Understanding the thermal evolution of Australian continental margin cover sequences accreted to the Banda Arc further constrains the maturation history, extent and rate of tectonic burial, mechanisms of deformation, and patterns and timing of collision-related exhumation. In this paper we use results from our investigation of peak paleotemperature (PPT) indicators and age data (apatite fission track and 40Ar/39Ar geochronology) to construct a temperature vs time model for the Australian continental margin and the Banda orogenic wedge. The thermal history model is important because it provides a way to test thermal responses predicted by various rival hypotheses about the kinematics and timing of the Banda arc–continent collision.

Kinematic models for the Banda Arc–continent collision differ in the extent of underthrusting of Australian continental margin cover sequences beneath the Banda forearc and processes of exhumation. Most structural reconstructions show Australian cover sequences underthrusting to increasingly greater depths along a north dipping subduction zone beneath the Banda forearc (Fitch and Hamilton, 1974; Hamilton, 1979, 1988; von der Borch, 1979; Barber, 1981; Audley-Charles and Harris, 1990; Charlton, 1991). Some of these models show depths of burial as great

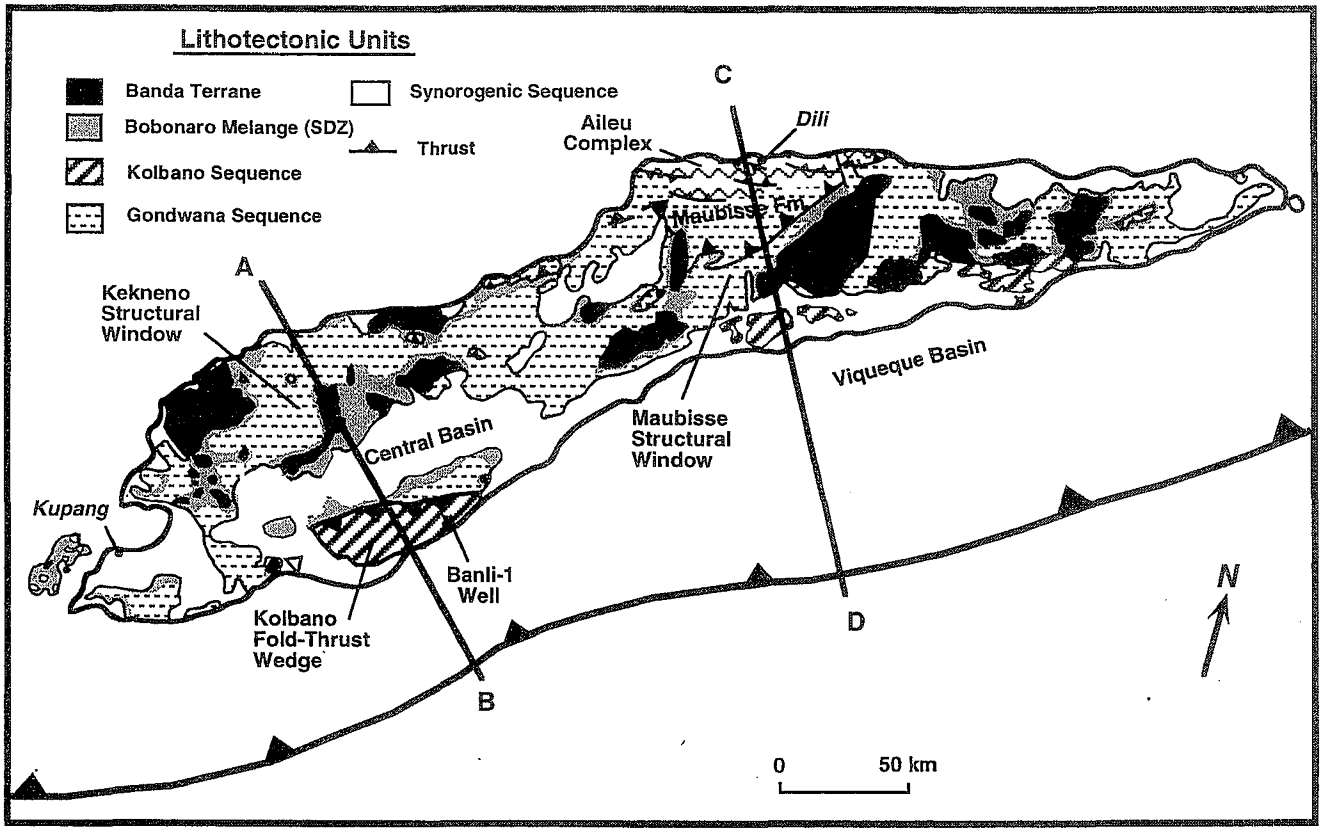

Fig. 2. Map of lithotectonic units of Timor island (after Harris et al., 1998). Nappes of Banda Terrane (black) are erosional remnants of the uppermost structural unit of Timor. The nappes are structurally underlain by the Sonnebait Disruption Zone (SDZ), a melange zone that separates units of Asian and Australian affinity.

as 40 km in the hinterland of the collision. Models for subsequent exhumation of these sequences involve plate rupture and rebound (Price and Audley-Charles, 1987; Charlton, 1992). However, the only possible evidence of such deep burial is a thin Barrovian metamorphic sequence found along the north coast in the Aileu Complex that yields pressure estimates of 5–7 kb (Berry and Grady, 1981). With the exception of the Aileu Complex, all other Australian affinity units exposed on Timor are not metamorphosed. An alternative kinematic model based on structural field mapping (Harris, 1991, 1992; Harris et al., 1998) and seismic reflection profiles (Snyder et al., 1996) shows that the accretionary wedge is doubly vergent (Figs. 2 and 3). Retro-wedge movement (arc-ward thrusting) in the hinterland allows accreted material to take a shallower path through the orogenic wedge, which requires much less exhumation. The model also accounts for incorporation of forearc thrust sheets and deep burial of some units. In this paper we analyze PPT indicators throughout the Timor orogenic wedge to better constrain the deformation path of rock units accreted from the Australian margin into the Banda forearc. The youth of the collision allows us to compare time vs temperature data from accreted units with equivalent units on the Australian Shelf. It also provides a unique advantage for constraining possible deformation pathways through the orogen.

The timing of PPT and accretion are additional topics of debate. Some suggest that the collision between the NW margin of Australia and the Banda forearc (Banda Terrane in Figs. 2 and 3) occurred before the Late Miocene to present arc–continent collision based on the 33–35 Ma metamorphic cooling age of the Banda Terrane (e.g. Helmers et al., 1989; Sopaheluwakan et al., 1989; Linthout et al., 1997). Cooling ages for the metamorphic rocks of the Aileu Complex range from 5–8 Ma (Berry and McDougal, 1986). Time vs temperature data for the bulk of units that form Timor is needed to constrain the age of accretion. We use apatite fission track geochronology in this study to investigate the timing of PPT and to develop a thermal history model for accreted Australian continental margin units. The model provides limits for pre- and syn-collisional PPT and ages of cooling, and relates the PPT pattern to structural features of the Australian continental margin and the Banda orogenic wedge.

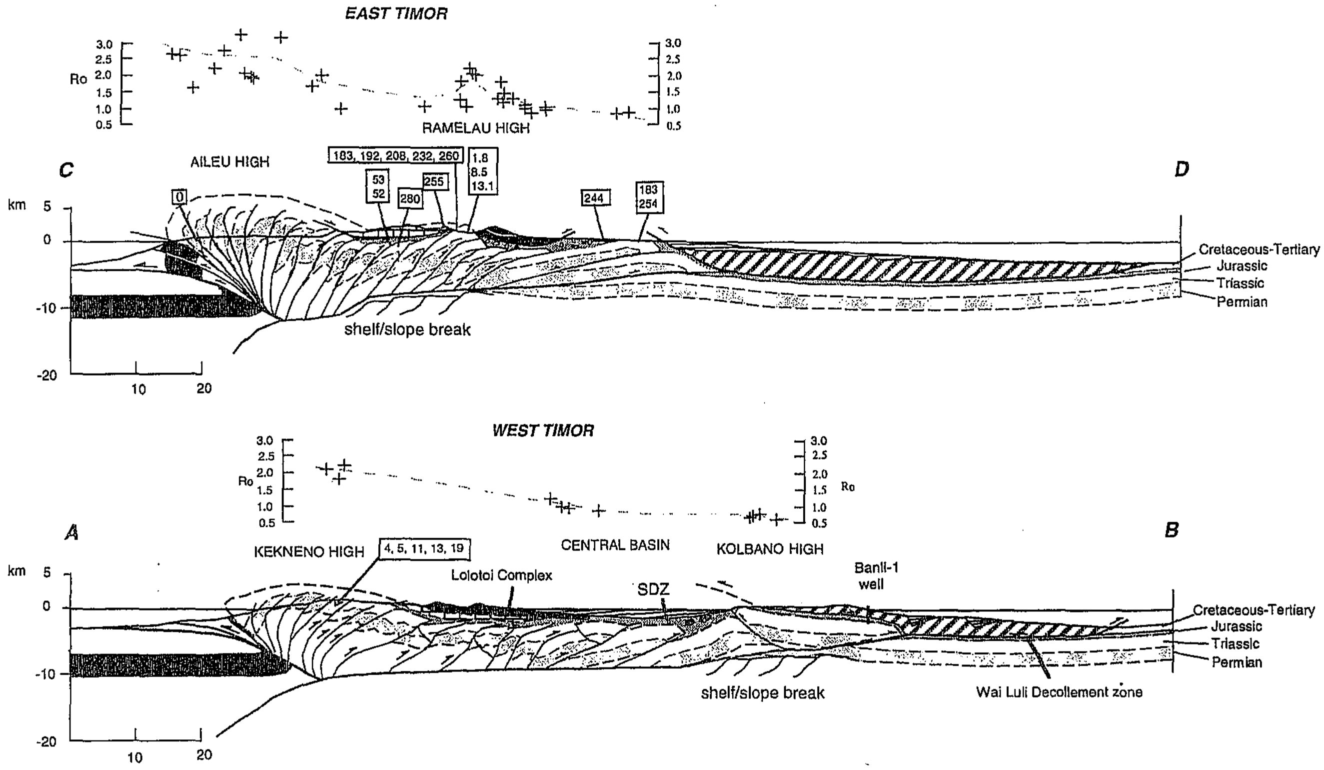

Fig. 3. Interpretative cross-sections through East and West Timor showing structural positions of fission track ages (in boxes) and % *Ro* values (see Fig. 2 for lines of section). The Banda Terrane nappe (black) structurally overlies the northern part of the orogenic wedge, but is detached from its roots. The roots of the Banda Terrane are structurally buried by the retro-wedge (zone of backthrusting). The Maubisse/Aileu thrust complex (brick pattern) and the Bobonaro melange (dark gray) structurally underlie the Banda Terrane. The Banda Terrane and Aileu/Maubisse thrust complexes rarely reach south of the Central and Viqueque Basins. Synorogenic sedimentary units in these basins unconformably overlie and are incorporated into the orogenic wedge. South of the Central Basin is the Kolbano fold and thrust belt (diagonal pattern), which is underlain by the Jurassic Wai Luli decollement zone (gray). % *Ro* values and apatite fission track ages show a general increase in values northward. Variations in this trend are found within structural windows where deeper units are exposed and with stratigraphic depth within individual thrust sheets.

2. Geologic overview

The island of Timor is an emergent portion of the Banda Arc–continent collisional suture zone, originating from Miocene to Present convergence and collision between the Australian passive continental margin and the Banda Arc-trench system. Geologic relations and tectonic reconstructions indicate that subduction initiated in the Timor region during the Middle Miocene (e.g. Kenyon, 1974; Hamilton, 1979; Bowin et al., 1980; Abbott and Chamalaun, 1981). At that time, Cretaceous-age Indian Ocean lithosphere attached to Australia subducted beneath the Banda forearc or Banda Terrane (Audley-Charles and Harris, 1990). By Late Miocene time, the more buoyant distal reaches of the Australian continental margin arrived at the trench in the Timor region, resulting in a transition from subduction to collision. Subsequently, the oblique Banda Arc–continent collision has propagated SW from Timor to its present position south of Sumba Island (Fig. 1). In a manner that is still poorly understood, sedimentary cover sequences of the NW Australian continental rise and slope accreted to the base and front of the Banda Terrane along multiple detachments to form the present Banda arc suture zone.

Three distinct lithotectonic units are exposed in the Banda Arc-Australian continent collision zone of the Timor region: the Banda Terrane of Asian affinity, and the Gondwana and Kolbano sequences of Australian affinity (Figs. 2–4). The Banda Terrane is a fragment of Banda forearc crust (upper plate of the arc–continent collision). It consists of the Lolotoi metamorphic complex, arc affinity volcanic rocks, and interbedded sedimentary layers. The mostly sedimentary Gondwana and Kolbano sequences were accreted beneath and in front (trenchward) of the Banda Terrane as the Australian passive continental margin collided with the Banda forearc. The Bobonaro melange is found in diapirs throughout the orogenic wedge and along the Sonnebait Disruption Zone (SDZ, Fig. 3), which is a low-angle thrust contact between the Banda Terrane and underlying Australian affinity units (Harris et al., 1998). Each of the lithotectonic units are stacked in a structural succession that

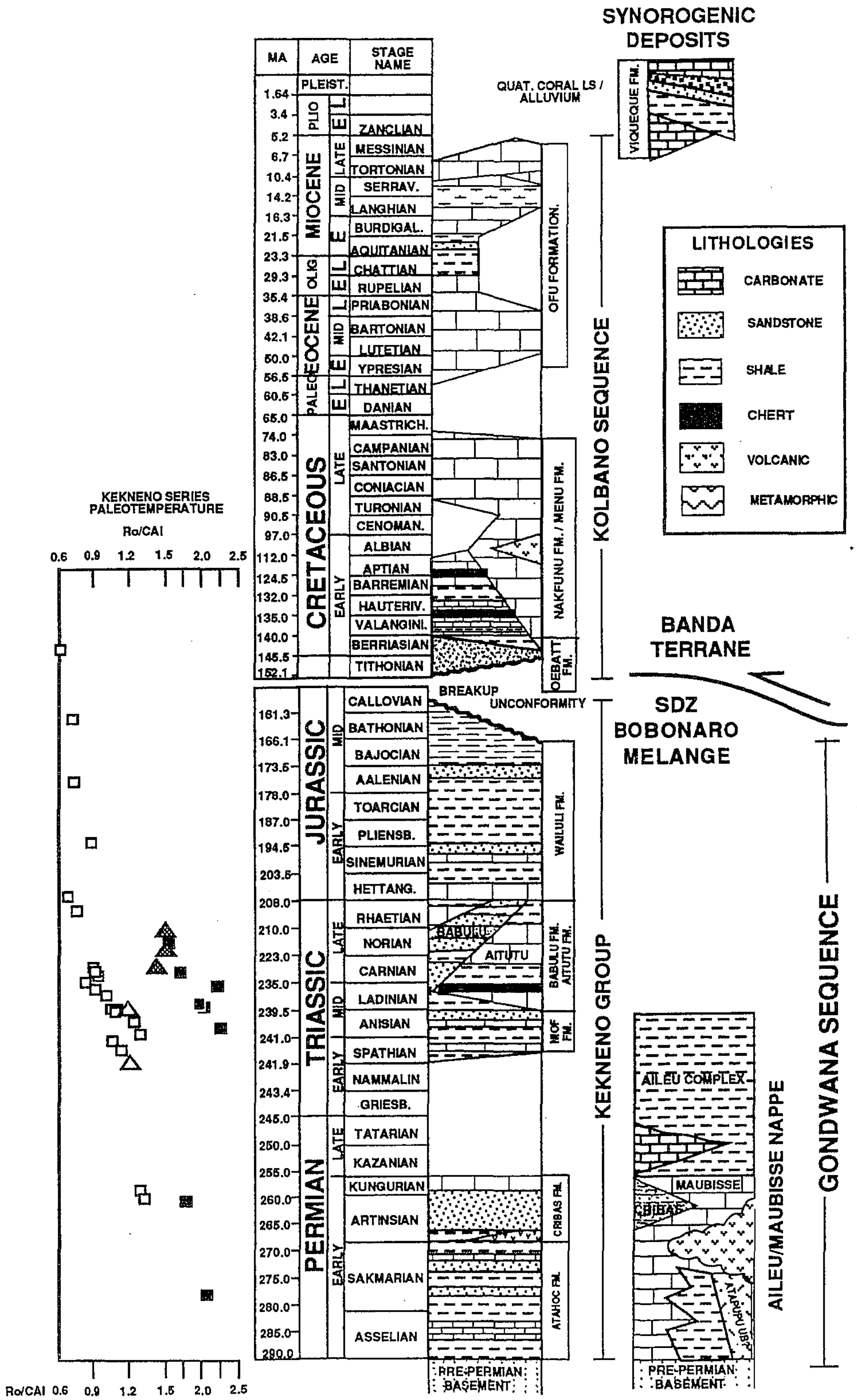

Fig. 4. Lithotectonic units of Timor and thermal maturity (*R*o/CAI) plotted according to stratigraphic depth. Boxes are *R*o values and triangles are CAI. Darkened symbols are values for samples that were overthrust by the Banda Terrane. Thermal maturity increases with depth and is offset by around 0.6 *R*o (~90°C higher temperature or 3.0–3.5 km of overburden) for units overthrust by the Banda Terrane.

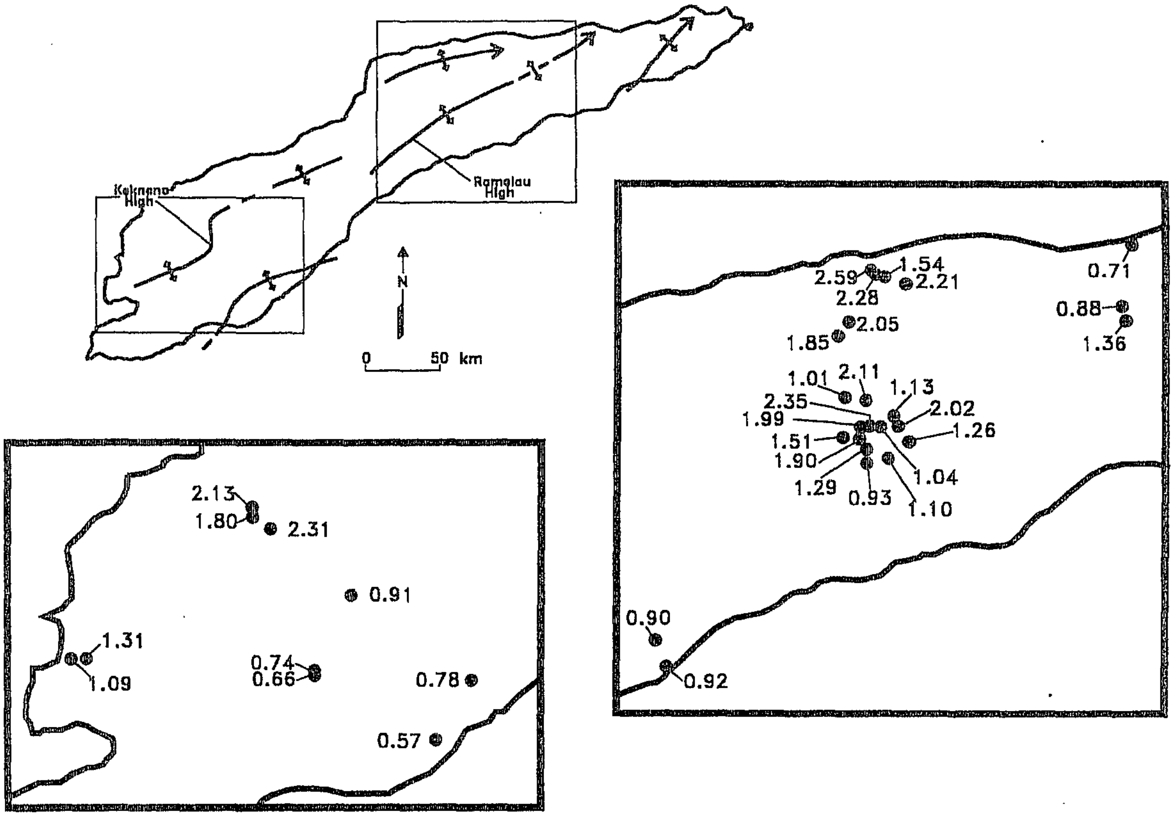

Fig. 5. Vitrinite reflection sample localities. Simplified structural reference map of Timor shows positions of structural highs that form the Ramelau/Kekneno Arch (RKA). These features are not simple anticlinoria, but rather structural culminations most likely positioned above major ramps along the basal decollement. Notice anomalously low values (0.7–1.3) along the western and eastern edges of northern Timor where average $Ro = 2.02$. Higher stratigraphic units are exposed in these parts of the north coast due to the plunging out of structural highs. The increase of Ro in easternmost Timor from the north coast toward the center of the island demonstrates the increase in stratigraphic depth toward the center of the Ramelau structural high.

intersects the present erosional surface of Timor Island at progressively deeper structural levels towards the north and center of the island (Figs. 3 and 4). Syncollisional sedimentary sequences lie unconformably over the suture zone assemblage.

PPT indicators used for this study were found in Permian to Jurassic units of the Kekneno Group (Simons, 1940; Audley-Charles, 1968), which is a facies of the Gondwana Sequence that is more proximal to the Australian craton. The Permian–Triassic Maubisse Formation and Aileu Complex represent more distal facies that are thrust over the Kekneno Group (Figs. 2–4). Each of these units was deposited in a North Sea-type extensional basin that formed on the northern Gondwana craton. The sedimentary source during this synrift extensional phase was mostly granitic and calc-alkaline volcanic rocks to the north (Audley-Charles, 1983; Bird and Cook, 1991). The source region was rifted away during Late Jurassic breakup of northern Gondwana to form the present NW Australian passive margin.

Post-breakup sedimentary units of the Kolbano Sequence that accumulated on the passive margin were sourced mostly from the Australian craton to the south. The Kolbano Sequence consists of a condensed series of Cretaceous to Late Tertiary pelagic mudstone, chert and calcilutite, which were deposited on the rapidly subsiding and drifting slope and rise of the NW Australian passive margin. These deposits thicken and become more carbonate-rich towards the continental shelf, and cause progressively deeper burial of the Kekneno Group towards the shelf.

As the NW Australian passive continental margin arrived at and began to underthrust the Java Trench in the Middle Miocene to the present, the Kolbano Sequence was the first to detach and formed an imbricate stack of thrust sheets above a decollement in clay-rich units at its base (Wai Luli Formation, Fig. 3). The thrust stack forms the Kolbano fold-thrust belt of southern West Timor (Figs. 2 and 3). The depth and character of the Wai Luli decollement is constrained by field mapping near the rear of Kolbano fold-thrust belt (Harris et al., 1998), drilling in Banli-1 well (Sani et al., 1995), and in seismic reflection profiles (Breen et al., 1986; Reed et al., 1986; Karig et al., 1987).

The bulk of the Gondwana Sequence underlies the

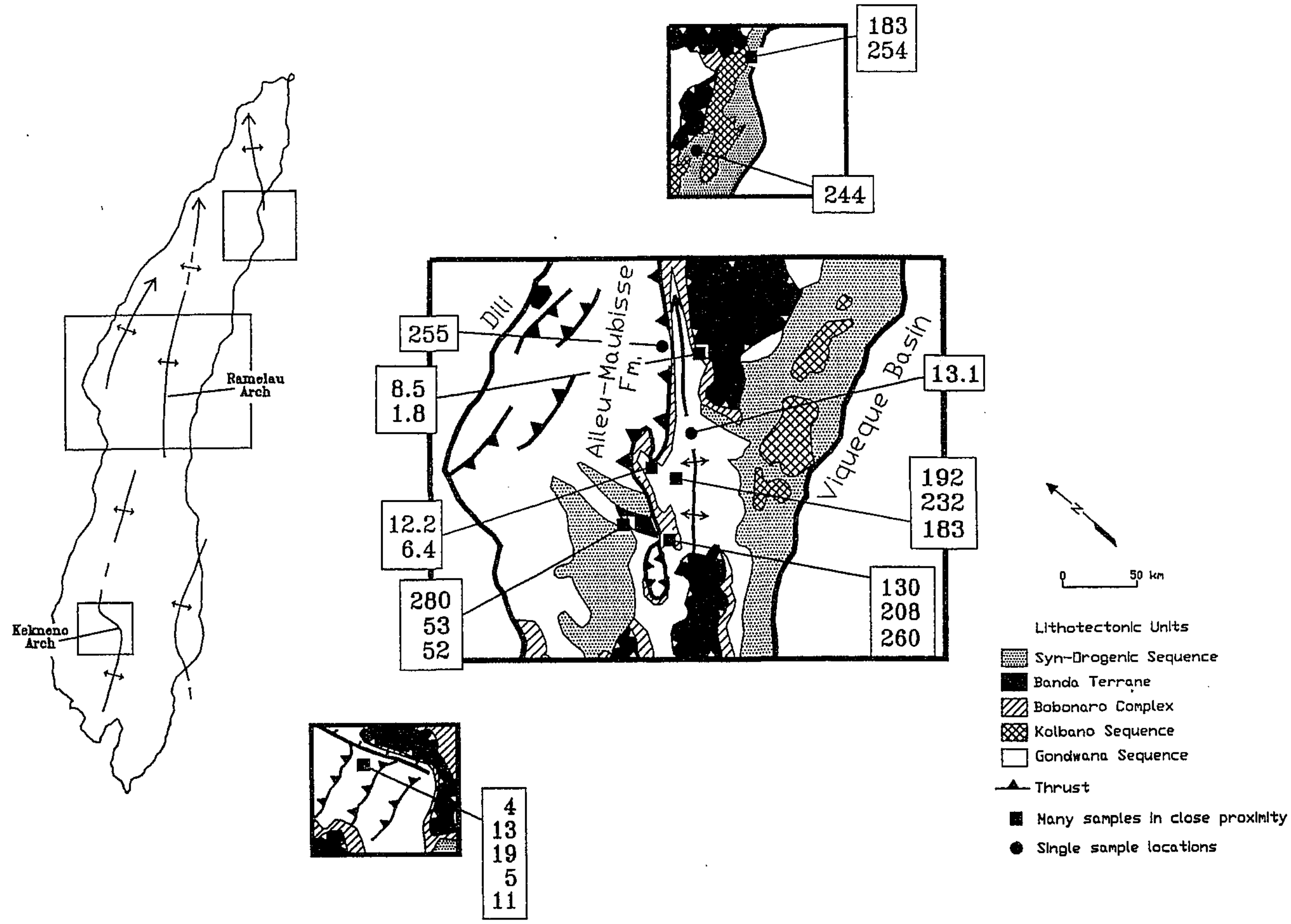

Fig. 6. Simplified geologic map showing fission track sample localities and corresponding ages. The oldest ages correspond to either structurally high units of distal parts of the continental margin (Maubisse Formation) or stratigraphically high units (Upper Triassic Babulu Formation) from proximal parts of the continental margin.

Wai Luli decollement zone, and was thrust beneath the Banda Terrane before it began to shorten above a basal Permian or lower decollement. The resulting contractional belt lifts lower Gondwana Sequence units to an elevation of nearly 3000 m along the Ramelau–Kekneno Arch (RKA). The RKA stretches from north of Kupang to the Kekneno region in West Timor and rises again as the Ramelau ridge (Aitutu and Basel anticlines) of central East Timor (Fig. 5). South of the RKA, isolated klippen of the Banda Terrane and Maubisse Formation are all that remain of the extensive roof thrust that covers the orogenic wedge in surrounding parts of the island and offshore along orogenic strike, see Fig. 6.

3. Peak temperatures

3.1. Present geothermal gradient

Heat flow measurements from wells drilled in the Aliambata, Suai and Kolbano regions (Fig. 2) of southern Timor indicate a present-day geothermal gradient of 25–30°C/km (Crostella, 1977; Sani et al., 1995). In some wells the gradient varies with depth from 15°C/km in shallow sections of synorogenic cover and Kolbano Sequence thrust units to 30°C/km at approximately 1200 m within and below the Wai Luli decollement (Sani et al., 1995).

Horstmann (1989) reports similar thermal gradients to those measured in Timor for the NW Australian Shelf. Data from 90 wells located throughout the NW Shelf show that most temperature gradients vary between 25 and 30°C/km. Wells in the Vulcan subbasin indicate horizontal variations in heat flow of a few degrees centigrade over distances of tens of kilometers. Other wells demonstrate some stratigraphic variation where shale units are more thermally altered.

These thermal gradients predict peak temperatures for the Gondwana sequence of 100–150°C with average burial depths on the Australian slope of rise of 2–3 km and 3–5 km for the shelf region. The estimates

Table 1
Vitrinite reflectance values (%*R*o)

Longitude	Latitude	*R*o
124.47	10.07	0.57
124.25	9.92	0.66
125.61	8.94	0.68
126.01	8.53	0.71
124.25	9.92	0.74
124.55	9.94	0.78
125.99	8.65	0.88
125.27	9.30	0.90
124.32	9.73	0.91
125.28	9.36	0.92
125.59	8.90	0.93
125.61	8.94	0.96
125.62	8.90	0.98
123.68	9.85	1.00
125.56	8.81	1.01
125.60	8.85	1.04
123.68	9.85	1.09
125.62	8.90	1.10
125.62	8.83	1.13
125.64	8.87	1.26
125.59	8.89	1.29
123.71	9.85	1.31
125.59	8.87	1.34
125.99	8.68	1.36
125.56	8.87	1.51
125.60	8.61	1.54
125.56	8.80	1.66
124.14	9.53	1.80
125.55	8.69	1.85
125.58	8.87	1.90
125.58	8.85	1.99
125.62	8.85	2.02
125.56	8.67	2.05
124.14	9.52	2.13
125.58	8.81	2.20
125.63	8.62	2.21
125.59	8.61	2.28
124.18	9.57	2.31
125.59	8.85	2.35
125.58	8.60	2.59
125.56	8.67	2.74
125.56	8.77	3.27
125.55	8.68	3.70

are similar to PPT measurements we conducted on Gondwana sequence units in Timor using vitrinite reflectance, conodont alteration and illite crystallinity.

3.2. Vitrinite reflectance

The degree of thermal maturation of vitrinite was estimated by measuring the mean reflectance, *R*o, according to quality standards set by Castano and Sparks (1974). Vitrinite is most abundant in fine-grained clastic rocks of the Gondwana Sequence, which yielded 43 samples with values ranging from 0.57 to 2.74% *R*o (Table 1). The distribution of values across the orogen shows an increase in *R*o at the RKA (Figs. 3–5). *R*o values south of the RKA gradually increase from 0.57% at the south coast to 1.31% near the arch axis. Values north of the RKA range from 0.71 to 2.74% according to stratigraphic depth. Within 5 km of the roughly defined axis of the RKA, most samples have *R*o values > 1.00%.

*R*o values are interpreted here on the basis of the distributed activation energy model of Burham and Sweeney (1989), which describes the evolution of *R*o through various heating times and temperatures. This model predicts *R*o values of 0.7–0.9% for Gondwana Sequence units on the present Australian Shelf exposed to temperatures of ~120°C (4–5 km burial depth at 27°C/km) for > 10 Ma. To achieve the *R*o values that are found throughout the hinterland part of the Timor orogenic wedge (1.20–2.74%) requires more heat than can be achieved by pre-accretionary stratigraphic burial alone. Either heat flow must be increased or some additional burial must be invoked (tectonic burial).

The Aileu Complex, which is found along the north coast of central Timor, has *R*o values that increase progressively from 0.96% near the RKA to 2.74% near the north coast (Figs. 4 and 5). The highest values are near the detection limit of the vitrinite reflectance method and indicate a PPT > 250°C for short heating times (< 10 Ma). Temperatures possibly as high as 450°C at 5.5 Ma ago are documented in metamorphic rocks in the Aileu Complex along the north coast by Berry and Grady (1981).

The trend of exposure to increasing paleotemperatures to the north in the Aileu Complex is opposite to that expected from the domal uplift pattern presented for Timor by de Smet et al. (1989). The observed pattern is more indicative of tectonic burial beneath an increasing thickness of accreted units, including the Banda Terrane, or by rift-related thermal events. Evidence for increased tectonic burial include the klippen of Banda Terrane that structurally overlie parts of the Aileu Complex and the collision-related penetrative ductile fabrics found throughout the Aileu Complex (Prasetyadi and Harris, 1996). Mapping and gravity measurements clearly indicate that these mostly metamorphic thrust sheets are not rooted, but may be at least 3 km thick in places (Chamalaun et al., 1976; Carter et al., 1976; Harris, 1992; Dropkin et al., 1993; Prasetyadi and Harris, 1996). Comparison of different balanced reconstructions along orogenic strike indicate that the Banda Terrane nappe thickened to the north (Fig. 3) and may have been 6–8 km thick prior to exhumation (Harris, 1991). The limited effective heating time associated with the Late Miocene tectonic burial event (< 10 Ma) requires temperatures > 150°C to increase *R*o values much above 1.00%. Low *R*o values do argue against structural reconstructions that thrust the entire forearc lithosphere over the hinterland accretionary wedge (Hamilton, 1979; Barber, 1981;

Charlton et al., 1991), which would cause much higher temperature and pressure conditions than those observed in the rock record.

More proximal units of the Gondwana Sequence that are interpreted to have been overlain by thinner parts of the Banda Terrane yield *R*o values between 0.71 and 2.31% (Fig. 3). These values generally increase with stratigraphic depth, although most values are higher than correlative units south of the RKA. The lowest *R*o values (0.57–0.78%) are found in the post-rift Kolbano Sequence, which further demonstrates a normal pattern of decreasing thermal maturation with stratigraphic depth in areas not overthrust by the Banda Terrane (Fig. 4). *R*o values from the Kolbano Sequence are similar to those reported by Marshallsea (1991) from correlative Cretaceous and Tertiary units drilled on the Australian continental shelf, which yielded *R*o values of $<0.8\%$ at a depth of 3.5 km. According to these results, there is little, if any, evidence for increased thermal maturation of rocks accreted to the front of the Banda Terrane or thrust beneath its thin southern edge in the southern part of Timor.

*R*o values also differ along the strike of the RKA in a manner that is consistent with the doubly plunging, periclinal geometry of the arch (Harris, 1991). Therefore, these data support the hypothesis that the degree of exhumation of tectonically buried Gondwana Sequence units decreases away from central Timor in both NE and SW directions along orogenic strike (Fig. 5).

3.3. Conodont alteration

Conodonts from six different sites of Triassic Kekneno Group limestone provide an additional estimate of the extent and pattern of thermal maturation in Timor. All of the samples that yielded conodonts are from Ladinian–Carnian age strata. Four samples were collected from the Maubisse structural window within the RKA of central East Timor, and Berry et al. (1984) report two samples from the northeast coast. Conodont Alteration Index (CAI) values for these samples range from 1.0 to 1.5 (Figs. 3 and 4), which indicates exposure to temperatures of ~80–140°C according to thermal models of Epstein et al. (1976) and Harris (1979). The greatest thermal alteration was found in samples from the core of the RKA, whereas the lowest values are from the northeastern plunging nose of the RKA. Although the data is sparse, the extent and pattern of peak thermal alteration is essentially the same as that indicated by the vitrinite reflectance study.

3.4. Metamorphism

Low to medium grade metamorphic rocks are found in both the Aileu Complex and Banda Terrane of the Timor hinterland region. These metamorphic complexes are most readily distinguished by differences in structural position, protolith, and thermal history. The Mutis/Lolotoi Complex of the Banda Terrane (Brown and Earle, 1983; Audley-Charles and Harris, 1990; Sopaheluwakan et al., 1989) is traceable to the west along orogenic strike into the Banda forearc basement of the Savu Basin (Harris, 1992). It has both continental and oceanic protoliths, and reached its thermal peak at or before 35–40 Ma (Dropkin et al., 1993). This metamorphic cooling age is interpreted by Sopaheluwakan et al. (1989) as the timing of thrust emplacement of the Banda Terrane over the Australian continental margin. However, there is no evidence that the passive margin of NW Australia was tectonically disturbed until the Late Miocene Banda Arc collision. Geochronological data from the Aileu Complex (Berry and McDougall, 1986) and Kekneno Group (this study) also support a Late Miocene to present age for collision of the Banda Terrane and the passive continental margin of Australia.

The Aileu Complex is composed mostly of metamorphosed pelites and psammites with local occurrences of carbonate and igneous bodies of Permian to Jurassic (?) age (Barber and Audley-Charles, 1976; Barber et al., 1977; Berry and Grady, 1981; Berry and McDougall, 1986; Harris, 1991; Prasetyadi and Harris, 1996). Most units are only slightly metamorphosed to sub-greenschist facies, except along the north coast where a steep metamorphic gradient abruptly increases the grade to amphibolite facies (Prasetyadi and Harris, 1996). Transitional stratigraphic relations between Aileu shale and limestone of the Maubisse Formation suggest that the Aileu Complex was the most distal part of the Gondwana Sequence (Barber and Audley-Charles, 1976; Prasetyadi and Harris,1996). The local occurrence of garnet/kyanite mineral assemblages in metapelites along parts of the north-central coast of Timor can be explained by proximity to the rift axis during Jurassic–Cretaceous continental breakup or by tectonic burial during Miocene arc–continent collision (Berry and McDougall, 1986). These assemblages yield critical radiometric age data that help constrain the timing of PPT. To what degree the rest of the Aileu Complex was heated is difficult to determine because its mineralogy (illite-chlorite and quartz) is insensitive to low grade metamorphic changes, with the exception of increases in reflectivity of vitrinite and crystallinity of illite.

Table 2
Apatite fission-track measurements and calculated ages for Timor samples[a]

								Dosimeter[b]		Spontaneous		Induced		Dispersion of age[c]		Central age[d]			
Sample	Location	Longitude (E)	Latitude (S)	Elevation (m) above sea level	Formation	Stratgraphic age (Ma)	No. X's	ρ_d	N_d	ρ_s	N_s	ρ_i	N_i	$P\chi^2$ %	R.E. %	Ma ($\pm 1\sigma$)	Mean track length (μm)	S.D. (μm)	No. of tracks
DH-90-001	Nenas	124.071	9.597	800	Babulu	208–230	15	1.426	9884	0.029	9	1.755	545	0	45	4 ± 1.5	too	few	tracks
DH-90-002	Nenas	124.069	9.600	780	Babulu	208–230	24	1.435	9884	0.038	35	1.749	1617	0	197	13 ± 6	too	few	tracks
DH-90-004	Nenas	124.074	9.594	850	Babulu	208–230	13	1.370	9884	0.100	26	2.543	659	0	155	19.2 ± 9.7	too	few	tracks
DH-90-005	Nenas	124.079	9.596	875	Niof	230–245	20	1.378	9884	0.284	18	1.860	1181	0	75	5.9 ± 1.7	too	few	tracks
DH-90-012	Nenas	124.083	9.599	880	Babulu	208–230	40	1.443	9884	0.069	79	2.099	2403	0	76	11 ± 2	too	few	tracks
DH-90-012	Cailaco	125.250	8.933	800	Undif. Triass	230–245	20	1.652	11153	0.191	216	0.191	216	75	0.07	280 ± 27	12.68 ± 0.33	1.53	23
DH-90-013	Cailaco	125.252	8.933	825	Undif. Triass	208–245	25	1.410	9884	0.273	199	2.302	1678	0	103	53 ± 12	too	few	tracks
DH-90-015	Cailaco	125.257	8.933	850	Undif. Triass	208–245	24	1.459	9884	0.198	321	2.11	3421	0	105	52 ± 12	12.14 ± 0.15	1.40	93
DH-90-020	Memo	125.248	9.023	700	Bobo	1.5–290	30	1.652	11153	0.576	789	1.398	1915	0	78	130 ± 20	10.55 ± 0.26	1.92	54
DH-90-021	Maliana	125.242	9.018	575	Aitutu	208–245	30	1.451	9884	0.637	761	0.807	964	< 1	35	208 ± 18	12.26 ± 0.18	1.34	58
DH-90-022	Babalai	125.236	9.012	550	Aitutu	208–245	30	1.643	11153	0.793	1343	0.901	1524	< 1	20	260 ± 15	12.02 ± 0.18	1.84	110
DH-90-023	Colimau	125.382	9.007	875	Undif. Triass	208–245	20	1.394	9884	0.942	751	1.158	923	< 1	20	192 ± 18	11.59 ± 0.18	1.77	100
DH-90-024A	Colimau	125.388	8.998	875	Undif. Triass	208–245	20	1.619	11153	0.488	291	0.589	351	60	13	232 ± 21	11.91 ± 0.26	1.74	45
DH-90-024B	Colimau	125.388	9.002	875	Undif. Triass	208–245	20	1.459	9884	0.522	410	0.664	522	0	36	197 ± 22	12.22 ± 0.19	1.58	72
DH-90-025	Colimau	125.422	8.921	1200	Undif. Triass	208–245	28	1.402	9884	0.081	66	2.577	2100	< 1	122	12.2 ± 3.4	12.12 ± 0.72	2.60	14
DH-90-026	Colimau	125.422	8.921	1200	Undif. Triass	208–245	30	1.624	11153	0.083	103	2.91	3624	< 1	163	6.4 ± 2.2	too	few	tracks
DH-90-0.43	Maubisse	125.621	8.852	1400	Aitutu	208–245	19	1.629	11153	0.058	27	2.895	1344	.0	112	8.5 ± 2.8	too	few	tracks
DH-90-050	Maubisse	125.585	8.874	1375	Babulu	208–230	36	1.386	9884	0.004	12	0.455	1557	86	1.6	1.8 ± 0.5	too	few	tracks
RH-90-045B	W. Aitutu	125.520	8.980	900	Babulu	208–230	20	1.633	11153	0.058	41	2.13	1483	0	121	13.1 ± 4.3 .	too	few	tracks
DH-90-053	W. Aitutu	125.590	8.840	1200	Maubisse	240–290	5	1.648	11153	1.964	196	2.305	230	60	21	255 ± 39	too	few	tracks
RH-90-060	Aliambata	126.600	8.800	60	Undif. Triass	208–245	20	1.362	9884	0.996	866	1.392	1210	< 1	30	184 ± 17	11.94 ± 0.16	1.56	94
RH-90-064	Aliambata	125.590	8.830	70	Undif. Triass	208–245	15	1.638	11153	1.595	1494	1.74	1630	< 1	33	254 ± 19	10.87 ± 0.18	1.77	100
RH-90-069C	Viqueque	126.370	8.830	125	Viqueque	L. Mioc.	16	1.354	9884	0.315	311	0.285	282	70	7	244 ± 21	14.14 ± 0.39	1.84	23

[a] Analyses by external detector method using 0.5 for the $4\pi/2\pi$ geometry correction factor;.

[b] ρ_d, ρ_s and ρ_i are track densities as measured and are ($\times 10^6$tr cm^{-2}); N_d and N_s and N_i are numbers of tracks counted;.

[c] $P\chi^2$ is probability of obtaining χ^2 value for ν degrees of freedom, where ν = no. crystals -1;.

[d] Central age is a modal age, weighted for different precisions of individul crystals (Galbraith and Laskett, 1993); [e]Ages calculated using dosimeter glass CN-5 for apatite with $\zeta_{CN5} = 347 \pm 5$ calibrated against multiple analyses of IUGS-recommended age standards (Hurford, 1990).

3.5. Illite crystallinity

Values of illite crystallinity, which increases with increasing PPT, were measured in clay-rich rocks from throughout Timor. Crystallinity is determined by dividing the height/width ratio of the 10Å illite peak by the same ratio of the 3.33Å quartz peak from X-ray diffractograms. In the Aileu Complex ($n = 12$) illite crystallinity values range from 0.647 on the north coast to 0.334 (10 km south of Dili) to 0.150 in the transition with the Maubisse Formation near the RKA. Within the RKA values range from 0.219–0.086 with a mean of 0.141 ($n = 18$). A pattern of increased crystallinity with stratigraphic depth was also found with mean values of 0.167 ($n = 5$) from the Maubisse Formation, 0.156 ($n = 5$) from the Aitutu Formation and 0.112 ($n = 9$) from the Upper Triassic, Jurassic and SDZ. These values attest to PPT mostly in the range of diagenesis with increasing values with stratigraphic and structural depth.

4. Age of thermal events

4.1. 40Ar/39Ar dating

Berry and Grady (1981) and Berry and McDougall (1986) studied metamorphic rocks of the Aileu Complex on the north coast of Timor and used K/Ar and 40Ar/39Ar dating techniques to identify two metamorphic events. The highest grade event is associated with a prograde metamorphic assemblage of upper amphibolite facies (>650°C) metapelites and amphibolites found in a narrow band along the north coast of central East Timor. A minimum cooling age of ~70 Ma is estimated from release spectra. These prograde high T–low P assemblages are overprinted by a medium P–medium to low T metamorphic event that completely reset the 40Ar/39Ar systematics of most amphibole and all mica samples along the north coast. Most of these minerals yield 40Ar/39Ar plateau ages of 8–9 Ma, which implies that these rocks cooled through the critical isotherm for Ar retentivity (350–560°C) at that time. This late Miocene date is contemporaneous with the age of the oldest synorogenic sedimentary rocks found in the Viqueque and Central Basins of south-central Timor (Audley-Charles, 1968, 1986; de Smet et al., 1989), which are commonly used to date the onset of the Banda orogeny. 40Ar/39Ar plateau ages from white mica show that the north coast region of the Aileu Complex had cooled to 350°C by 5.5 Ma, which yields exhumation rates (uplift and denudation) of around 3–5 mm/year, assuming present geothermal gradients.

We attribute the medium to low temperature Neogene metamorphic event to tectonic burial deep in the hinterland of the Banda orogen between around 12–5 Ma. This implies a limited heating time of <7 m.y. in a tectonic setting of known thermal disequalibrium, where temperatures may be much cooler at depth than expected. This interpretation is supported by the general pattern of increasing thermal maturity northward from the RKA. In detail, the thermal alteration pattern is much more complex and displays many abrupt changes that in some cases relate directly to the position of faults (Prasetyadi and Harris, 1996).

It is also possible that the Banda volcanic arc has thermally disturbed the Aileu Complex, since it is as close as 30–40 km in places. The simultaneous age of arc volcanism and underthrusting make it difficult to distinguish between the two possibilities. However, the lack of any intrusive rocks associated with the volcanic arc in the Aileu Complex make the possibility of arc heat metamorphism more remote.

4.2. Apatite fission-track analysis

Fission-track (FT) analysis of detrital apatite grains found in the Gondwana Sequence provide constraints for the thermal history of accreted materials at temperatures below ~110°C. Samples were collected throughout East Timor and in the Kekneno window of the RKA of West Timor, twenty-three of which yielded apatite (Table 2). The majority of the samples are from sandstone horizons in the Triassic Aitutu, Babulu and Niof Formations of the Kekneno Group (Figs. 4 and 6). In addition, results were obtained from an early Pliocene sandstone of the Banda Synorogenic Sequence, one igneous samples from the Maubisse Formation, and three from melange in the SDZ. The igneous sample is from a volcanogenic siltstone in a klippe of Maubisse Formation. The SDZ lies at the structural base of this klippe. Collectively these samples represent each of the stratigraphic intervals of the Gondwana Sequence: three different structural levels above, within, and below the SDZ, and deposits shed from the orogen itself.

The samples were prepared and analyzed at the London Fission Track Research Group according to methods detailed in Gleadow (1981), Hurford and Green (1982, 1983) and Storey et al. (1996). Samples were irradiated in the thermal facility of the Hifar Reactor at Lucas Heights, Australia.

4.3. Annealing of apatite fission tracks

All fission tracks in apatite are produced with the same track length of ~16.3 μm. Below about 60°C, tracks are stable over geological time periods, although some slight shortening does occur. Apatite within this stable zone accumulates tracks with negligible annealing, producing a narrow, symmetrical distribution of long tracks, with a mean length of 14–15 μm. Above ~60°C the tracks are annealed or shortened to a length controlled by the amount and duration of heating. Above temperatures of around 110–120°C apatite fission tracks are totally annealed and the age completely reset at geologic times of about 1 m.y. or more. A partial-annealing zone (PAZ) occurs between 60 and 120°C where pre-existing or newly formed tracks are shortened and an inherited age partially reset. The passage of an apatite into the PAZ, its residence time at different temperatures, and the time of emergence to cooler, track-stable temperatures will be recorded by the shortening of existing fission tracks, which are formed continuously throughout the thermal history. The distribution of track lengths thus provides an integrated record of the thermal history of a sample at typical upper crustal temperatures (Gleadow et al.,

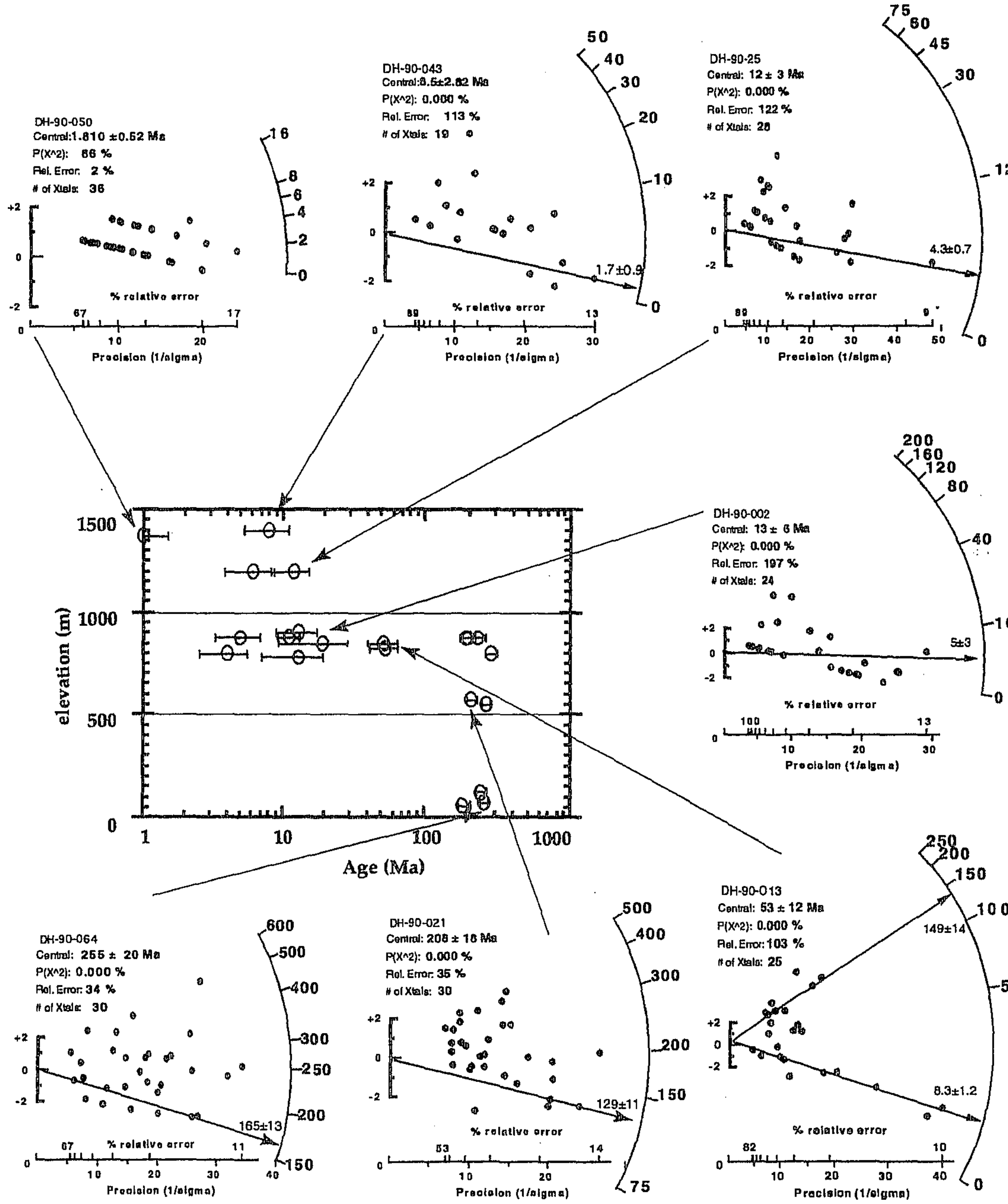

Fig. 7. Apatite fission track ages vs elevation. The trend of decreasing age with elevation is discussed in the text. Also shown are radial plots for representative samples. Radial plots present single grain ages and their associated precisions (Galbraith, 1990). Standard error for each point is given in the y direction. The x scale provides the approximate percent relative standard error of ages for each sample.

1986a,b). Such thermal histories may record either the progressive cooling of basement samples from high crustal temperatures, or the complete or partial resetting of inherited FT records of detrital apatite in clastic sediments through heating due to burial or an increase in geothermal gradient. Cooling is the consequence of denudation and unroofing of a sample, through a combination of surface and tectonic processes.

4.4. Fission track results: age groups and track lengths

Apatite FT central ages (modal age weighted for different precisions of individual crystals) for Timor samples range from 1.8 ± 0.5 to 280 ± 27 Ma (Table 2). Ages cluster distinctively into either Neogene or Gondwana Sequence (Permian to Jurassic) groups, with three samples of intermediate age. The dispersion of the single-grain ages as indicated by the χ^2 probability and age relative errors (Galbraith and Laslett, 1993) varies between homogeneous (e.g. DH-90-050 $\chi^2 = 86\%$, RE < 2) and highly heterogeneous (e.g. DH-90-021 $\chi^2 = < 1\%$, RE 35%). Confined track length distributions show mean track lengths of ~12 μm with standard deviations ~1.6 μm with fairly broad, negatively skewed unimodal distributions (Fig. 8).

The older group of ages comprises 10 samples whose apatite FT central ages vary between 184 ± 17 and 280 ± 27 Ma. All samples of this group, which were collected from the upper part of the Kekneno Group, occur at less than 1000 m elevation (Fig. 7). Most of these samples have the most dispersion of single-grain ages (Fig. 7).

Neogene Group FT central ages range from 1.8 ± 0.5 to 19.2 ± 9.7 Ma. All of these samples are from Kekneno Group sandstone layers that outcrop within 5 km of the RKA at elevations between 780–880 m in West Timor and 900–1440 m in East Timor. Single-crystal ages for all of these samples are extremely heterogeneous, with dispersion indices showing $\chi^2 < 1\%$ and relative errors often >100%. Sample DH-90-050 is an exception, having the youngest central age of 1.8 ± 0.5 Ma and homogeneous single-grain ages. Radial plots for these samples show less dispersion than the older group (Fig. 7). The young ages of these samples may result from low spontaneous track densities which, in turn, means that horizontal confined track lengths are exceedingly rare. Only one sample from this group (DH-90-025) yielded sufficient confined tracks to analyze, giving a mean length of 12.12 ± 0.72 μm with a broad distribution (Fig. 8).

Three samples with intermediate ages all derive from melange within the SDZ. Two samples from broken formation (transition from undisrupted strata to block in clay melange) yield apatite central ages of 53 ± 12 and 52 ± 12 Ma. Only one of these, sample DH-90-015, contained confined tracks that yield a mean track length of 12.14 ± 0.15 μm (Fig. 8). Sample DH-90-020 is from a block in melange that yielded an age of 130 ± 20 Ma and a mean track length of 10.55 ± 0.26 μm, which is the shortest confined mean track length of this study. Each of these intermediate age samples showed very inhomogeneous single-grain ages with $\chi^2 = 0$, although each is also characterized by two different linear trends of single grain ages (sample DH-90-013, Fig. 7). All of these samples that produced an intermediate mixed age are from an intermediate structural position within the Timor orogenic wedge.

5. Discussion

The wide difference in calculated central and single-grain ages for detrital apatite from Timor of approximately similar depositional age indicates either major differences of provenance and/or post-depositional thermal history. For samples with older apatite FT ages, the range of central ages (184–280 Ma) broadly coincides with the sediment stratigraphic ages (~208–290 Ma), although there are many grains in these samples that are much older than the age of deposition (Fig. 7). If the central ages are mostly provenance ages then the source for the apatite must have been broadly synchronous with deposition. Coeval volcanism or a hinterland that was rapidly cooling and eroding could each supply the sediment depocenter with detrital apatite having an approximate zero age, resulting in the FT ages measured today. Alternatively, the incorporation into sediment of detrital apatite whose ages significantly pre-date deposition would require substantial post-depositional annealing of the inherited tracks, resulting in a measured age fortuitously similar to the stratigraphic age of the sediment. Each scenario satisfies the measured FT age criteria. However, the track length profiles would be different for the two possibilities. For apatite derived from a synchronous provenance there would be minimal post-depositional annealing in order to maintain the age; track lengths should thus be long (13.5–14 μm) with a narrow distribution. Single-grain ages should also be similar giving a low factor of dispersion. Where post-depositional annealing of inherited age is invoked, track length patterns will be more complex, generally broader with reduced mean track length values. Single-grain age values would also be more inhomogeneous. The age and length values measured for the "older" group of samples show close similarities with the characteristics of the second scenario suggesting that these samples contain apatite with inherited histories that have experienced some post-depositional annealing (e.g. O'Sullivan and Parrish, 1995).

For the younger apatite age group, the dramatic resetting of the central ages indicates substantial post-depositional annealing. However, the heterogeneity of single-grain ages shows some residual older ages, occasionally up to 200 Ma (e.g. DH-90-002) implying that for a few crystals in some samples temperatures have been insufficient to cause total annealing. Only one sample, DH-90-050 with a central age of 1.8 ± 0.5 Ma, shows a fully homogeneous single-grain age distribution.

The samples with intermediate ages reveal a clear bimodality in their single age distributions, having

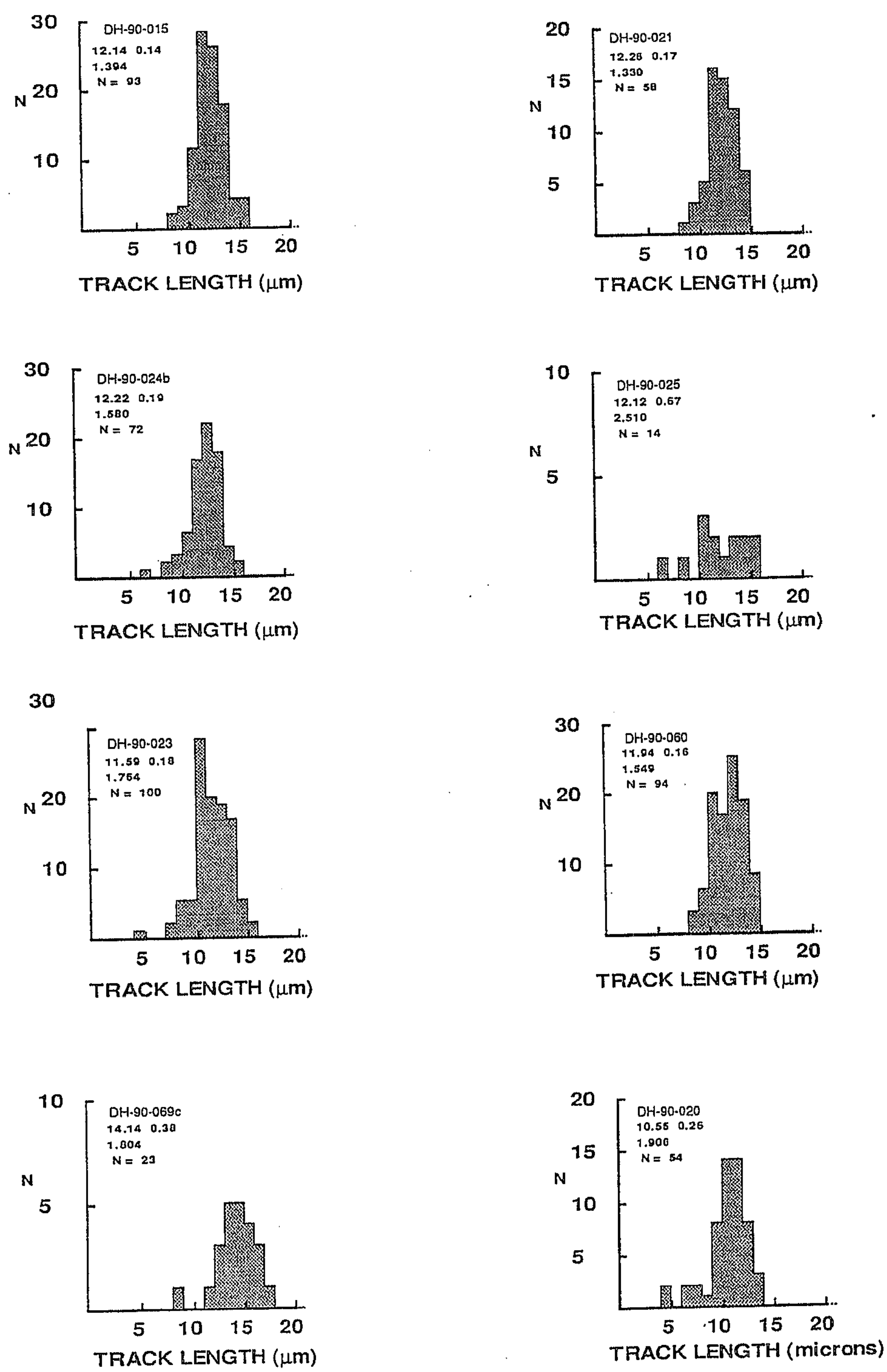

Fig. 8. Apatite track length distributions for all samples with horizontal confined tracks. Values in upper right are sample number, mean track length $\pm 1\ \sigma$ (μm), standard deviation (μm), and number of measured samples.

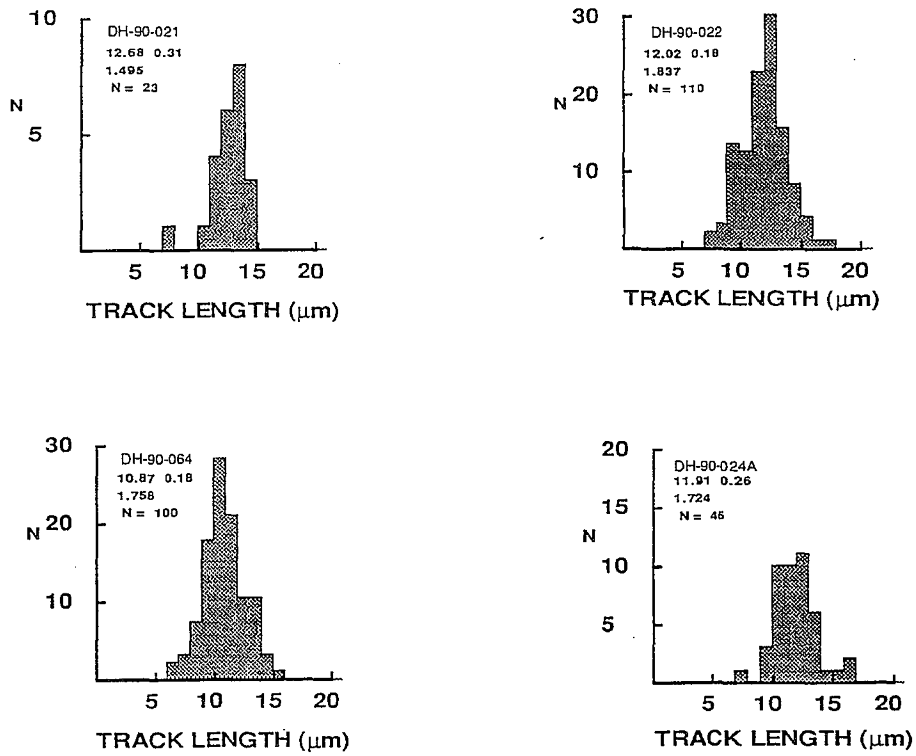

Fig. 8 (*continued*)

well-defined lower modes of Upper Miocene age (sample DH-90-013, Fig. 7). Those apatite grains recording this age must have been at temperatures sufficient to cause total FT annealing at that time, or very shortly before it. Those grains recording an older age appear to have experienced maximum annealing at a much earlier time, possibly in the Eocene or even Cretaceous. Microprobe analysis of sample DH-90-013 revealed that apatite defining the younger age mode were dominantly fluor-apatite in composition (1.5–2.0 wt % F) with negligible chlorine content. In contrast, those grains having the older ages contained < 1 wt % F and 1–2 wt % Cl. This correlation of older age with higher chlorine content implies a higher resistance of the chlorine-rich apatite to FT annealing, a relationship previously observed (Green et al., 1989). These samples of intermediate age thus appear to represent an intermediate position in the overall thermal history recorded by apatite FT analysis, with an Upper Miocene age component correlating with the Upper Miocene–Pliocene central ages measured for the younger group.

Generalized qualitative interpretation of the FT age and length data argue that, for the samples of younger age group, substantial, in many cases total, post-depositional annealing has occurred with cooling from within the PAZ being very recent. For the older age group, the length patterns indicate some modest annealing has occurred, but the absence of significant numbers of long tracks again suggests cooling from the PAZ to be late Cenozoic. The young age mode of the intermediate age group similarly argues for a late Miocene–Pliocene cooling. From the FT evidence the implication is that all samples have undergone broadly similar thermal histories but have experienced different thermal maxima.

6. Track-length distribution models

A numerical modeling procedure has been used to refine the thermal histories of four representative samples, using the measured data themselves to drive the modeling process rather than biasing the result by testing only restricted, pre-selected time–temperature histories. A Monte Carlo simulation, or probabilistic approach was used to select time–temperature points from within broadly-defined bounds, this thermal history being used to predict FT parameters using the Durango fission-track annealing algorithm of Laslett et al. (1987). The predicted track values were quantitatively compared to the observed values. Those thermal histories whose predictions agreed more closely with the observations were deemed more probable. Maximum likelihood was used, each track length and single-grain age observation being considered. The simulation process was repeated 10 times, with the selection procedure progressively biased to the more

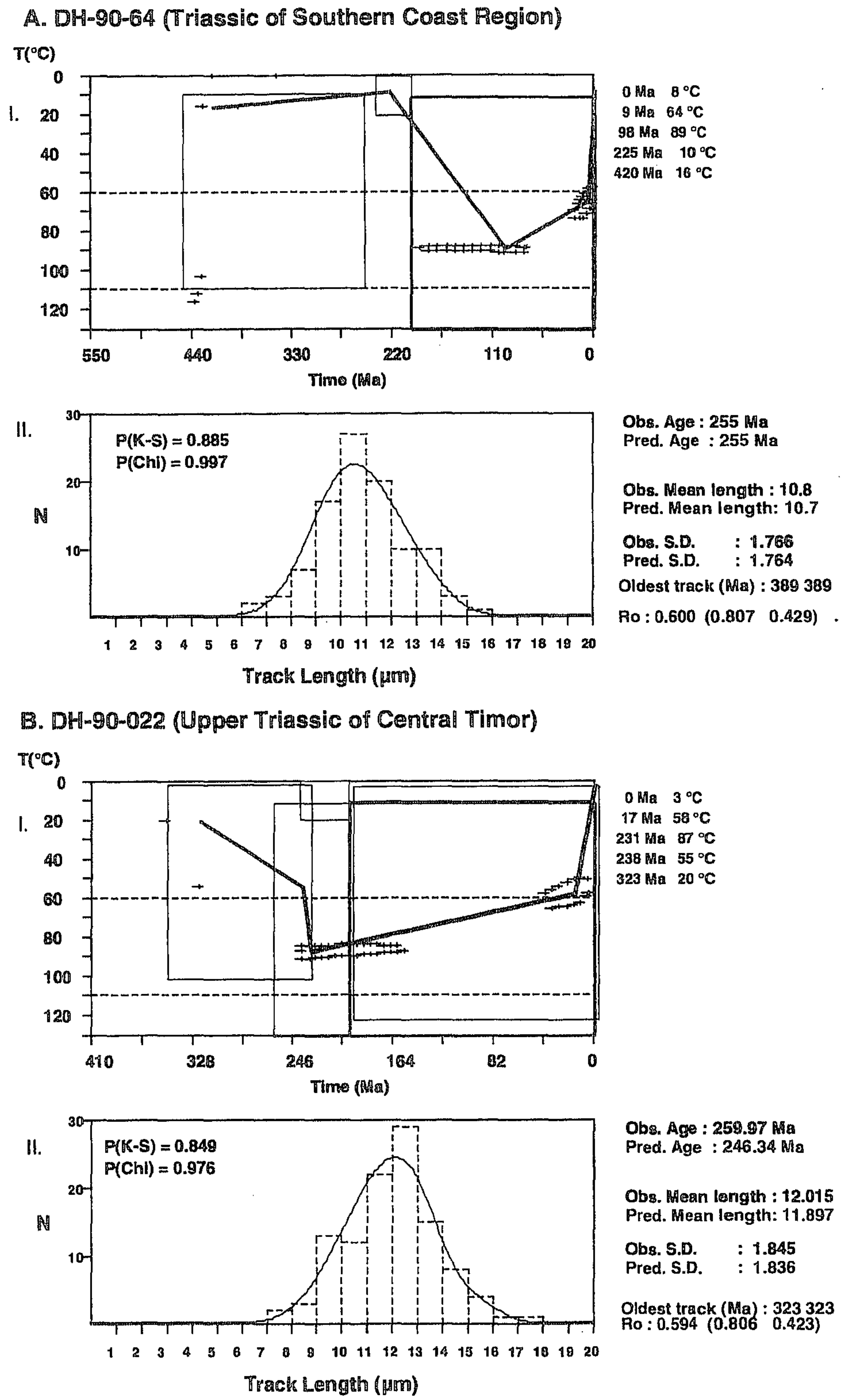

Fig. 9. Temperature vs time models for four samples from central andsouthern Timor. The models were generated using the approach of Gallagher (1995). Parts (I) show the 'best fit' thermal history, in bold, that produces the predicted results in (II). The bounds of other thermal histories that fit the observed apatite age and length data are shown as crosses. Boxes correspond to input parameters. Dashed libes correspond to the PAZ Parts (II) compare the track length distribution predicted by the best fit time–temperature history and observed.

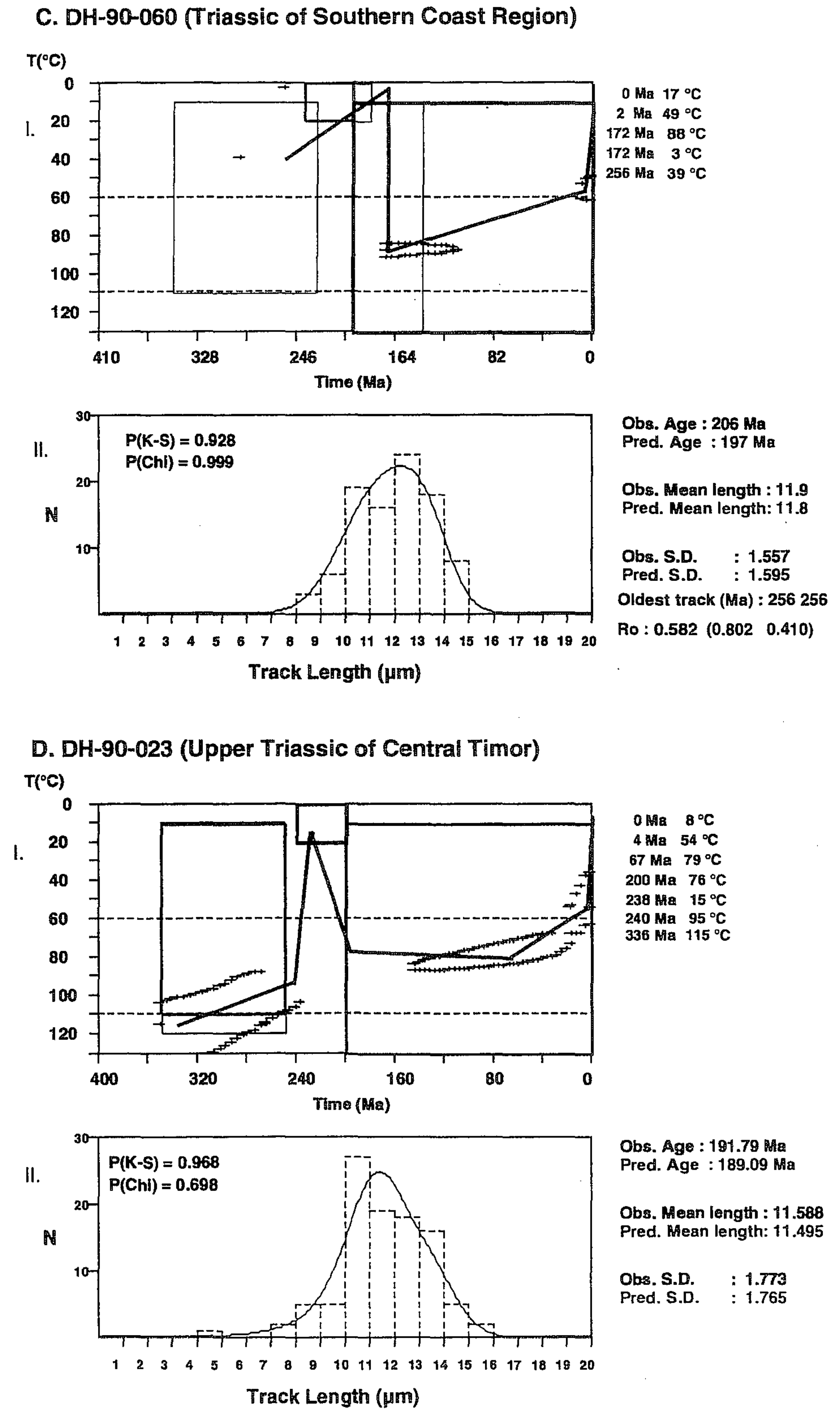

Fig. 9 (*continued*)

probable thermal histories. Initial selection of time–temperature points was random, but subsequently utilized a genetic algorithm (Gallagher, 1995). A total of 2000 thermal histories were tested for each sample.

The preferred genetic algorithm thermal history was tested to ensure that it was the local best solution by searching around each individual time–temperature point using a multi-dimensional line search technique to find the local maximum in the likelihood function, the 95% confidence region being defined as an ellipse in Fig. 9 (see Gallagher, 1995).

The modeling approach could only be used where an adequate track length data-set existed and was thus restricted to those samples of the older age group. Although the detail of thermal history differs in each case, in particular that before deposition, two key factors are common to each prediction:

1. The greater part of time since deposition has been spent in the PAZ at temperatures <90°C,
2. Cooling to temperatures below the PAZ occurred in the Late Miocene–Pliocene,
3. Unbiased quantitative modeling based upon the description of apatite annealing thus substantiates the original interpretation of the data.

7. Apatite provenance

Sample DH-90-053 from the older age group is a volcanic rock within the Permian Maubisse Formation, which yielded an apatite FT central age of 255 ± 39 Ma. Sandstone in the group is mostly feldspathic litharenites with abundant volcanic rock fragments. Analysis of modes of detrital framework grains shows similarities with the recycled orogen and arc orogen provenance fields of Dickinson (1985). It is possible that the source of the apatite for these samples may also be an igneous or metamorphic terrane of Permian age. Paleogeographic reconstructions of the Timor region during Permian–Triassic time interpret it as an intra-cratonic basin that was receiving siliciclastics from a convergent margin to the north and possibly from basement blocks to the south (Audley-Charles, 1983, 1988; Metcalfe, 1988; Audley-Charles and Harris, 1990). Permian and Carboniferous strata drilled in the Canning Basin of the NW Australian shelf to the southeast of Timor (Gleadow and Duddy, 1984) mostly yield apatite FT ages within the same range, 191 ± 10 to 298 ± 16 Ma) as those from the oldest group of Timor ages.

Sample RH-90-069C is of Lower Pliocene Viqueque Formation and yielded a Late Permian apatite FT central age of 244 ± 21 Ma. This sandstone was deposited as a turbidite shed from an emergent part of the Timor orogenic wedge to the north. Syncollision erosional and depositional patterns in Timor indicate that detrital apatite in Viqueque Formation sandstone is derived from high-level thrust sheets of mostly Gondwana Sequence units. In younger parts of the orogenic wedge, similar in developmental stage to Pliocene Timor, surface exposures of Permian–Triassic Kekneno Group and Maubisse Formation abound (Harris, 1991) and two samples from these have yield apatite fission track ages of 184 ± 17 and 254 ± 19 Ma. Therefore, we propose that the apatite in the Viqueque Formation was derived from the same high-level thrust sheets that yield old ages. The source for these apatite grains has since been eroded from above regions that now expose rocks of older stratigraphic age, but contain young mixed apatite ages.

8. Structural inversion

As rocks in the PAZ are brought to the surface in a coherent block, they preserve an age vs depth relationship that is reflected in age and track length variations with elevation. Rocks exhumed from upper levels in the PAZ yield older ages and longer mean track lengths than those from progressively lower levels, which produces a characteristic positive slope on plots of age vs elevation (e.g. Fitzgerald and Gleadow, 1990; Omar et al., 1994). A pattern of decreasing FT age and track length with depth is also found in wells drilled on the NW Australian continental margin (Gleadow and Duddy, 1984; Marshallsea, 1991). However, this trend is reversed in Timor, where samples of Triassic sandstone at high elevations have younger FT ages than those near sea level. The variation of age with elevation in Timor produces a steep negative slope (Fig. 7). The timing of accelerated cooling, which may be determined from abrupt changes in the slope of the age vs elevation plot, is not evident in the data of this study.

Fig. 7 clearly shows that with increased elevation, samples of broadly similar Triassic stratigraphic age have undergone progressively higher levels of track annealing. This is illustrated not only by the sequence of FT central ages, but perhaps more graphically by the representative examples of distributions of single-grain age radial plots (Fig. 7). For the lower and middle elevation older group samples, single-grain age populations are disparate. Higher and middle elevation younger group samples are also generally disparate, showing total annealing of crystals at different times. The highest sample, DH-90-050 gives the youngest central age of 1.8 ± 0.5 Ma, a homogeneous single-crystal age population and shows total resetting of all crystals at this time. The intermediate age samples also occupy an intermediate elevation, and here the bimodal single-grain ages reveal total resetting at an age comparable with that indicated for the youngest group.

It is highly improbable that this regional picture of higher temperatures at higher elevations could be explained by erosive denudation and thus some tectonic mechanism must be invoked. Basin inversion, where deeper-seated basinal sedimentary units are "raised" and shoved over shallower, basin margin sediments, or thrust stacking of distal parts of the Australian continental margin over more proximal ones, each proffer plausible mechanisms.

Two specific examples of the inverted age/elevation pattern occur in East Timor. DH-90-024A and B were collected in a river bed at an elevation of 832 m and yields ages of 232 ± 21 and 197 ± 22 Ma. DH-90-025 was collected from the ridge adjacent to the river at an elevation of 1200 m and yields an age of 12 Ma. Another example occurred at sample locations 012, 013 and 015. Sample 012 was collected in Kekneno Group units below the SDZ and yields an age of 280 ± 27 Ma. Samples 013 and 015 are within the SDZ, are 25 and 50 m higher in elevation, respectively, but yield intermediate ages of $52–53 \pm 12$ Ma. This abrupt change in age over such a short distance is difficult to explain with steep thermal gradients and is most likely a function of fault or diapiric juxtaposition of rocks of similar stratigraphic age, but with different thermal maxima.

An alternative hypothesis is that the abrupt age changes reflect thermal anomalies associated with the SDZ. For instance, hot springs are found within the SDZ near the locations that yield intermediate ages (Prasetyadi and Harris, 1996) and could, therefore, have resulted in partial resetting. However, there are also sample locations that yield older ages (DH-90-12) within decimeters of the hot springs. Apart from these hydrothermal systems, there is no evidence for local thermal anomalies associated with magmatic activity since the Cretaceous. Therefore, the most likely explanation for reverse age vs elevation relations remains contractional deformation associated with Neogene arc-continent collision and the development of the RKA.

9. Variations in the stratigraphic depth of the PAZ

Most of the Permian to Jurassic sequences drilled on the Australian Shelf (Gleadow and Duddy, 1984; Marshallsea, 1991) and in Irian Jaya (Weiland and Cloos, 1996) yield apatite FT ages similar to the Neogene age group found in this study. Apatite FT ages similar to stratigraphic ages in this region is rare. The difference between the older (Gondwana) age group and the highly-annealed apatite found in this study may result from pre-collisional differences in depth of stratigraphic burial on the passive margin of Australia.

Drilling and seismic reflection profiles of the pre-collision Australian margin to the south and west of the Banda orogen show that syn- and post-breakup sedimentary cover of the Kolbano Sequence thickens significantly towards the Australian Shelf. In most places along the shelf the break-up unconformity and underlying Gondwana Sequence are buried 2–3 km deeper than on the slope and rise of the passive margin (Fig. 10). Therefore the PAZ on the shelf is at a much higher stratigraphic level (Cretaceous to Tertiary) than on the slope and rise (within the Gondwana Sequence). Due to the fact that the PAZ is a function of depth and thermal gradient, it slopes up strati-

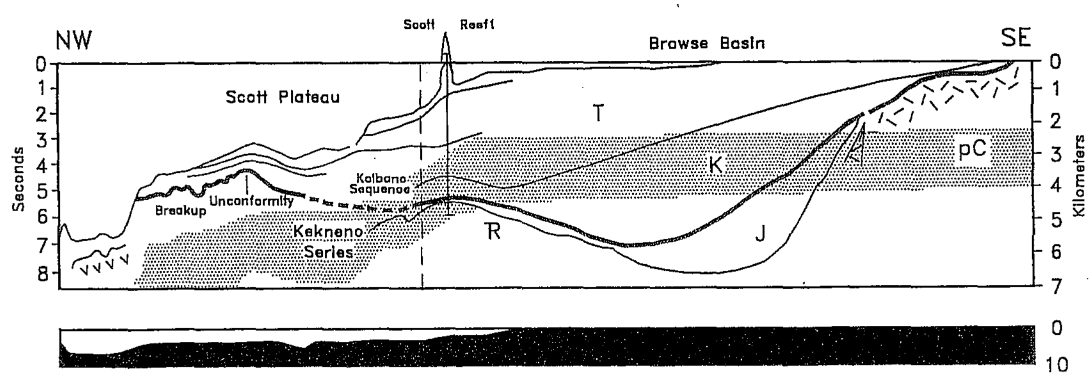

Fig. 10. Interpreted depth of partial-annealing zone (PAZ), shown in gray, on the Australian passive continental margin west of Timor. Modified from interpreted seismic reflection profile from Veevers et al. (1974). Units equivalent to the Kolbano Sequence and Kekneno Series are shown. Thinning of post-rift sedimentary cover associated with the transition from shelf to slope corresponds with a stratigraphic deepening of the PAZ toward the continental slope. The lower profile is the same section of the true scale.

graphic section toward the shelf. Estimates of the depth to the top and bottom of the present-day PAZ are possible using the average geothermal gradient (25°C/km) measured in offshore wells from the NW Australian shelf (Marshallsea, 1991). Seismic profiles of the NW Australian passive margin predict that the present-day PAZ moves from near the break-up unconformity at the shelf-slope break (Scott Reef-1) to near the base of the Kekneno Group in more distal portions of the slope. The horizontal separation between the top and bottom of the PAZ may be as little as 100 km (Fig. 10).

One location in Timor where older fission track ages were found structurally above younger ones, is attributed to these differences in the stratigraphic depth of the PAZ. In the Maubisse region a klippe of the Permian Maubisse Formation structurally overlies siliciclastics of the Kekneno Group along the SDZ. Volcanogenic material within the Maubisse Formation yields an age of 255 ± 39 Ma. Apatite from the siliciclastics at the structural base of the Maubisse klippe yields an age of 8.5 ± 2.8 Ma. Most structural reconstructions of the Banda orogen interpret the Maubisse Nappe as rootless and far-travelled from a distal position on the Australian margin (Carter et al., 1976; Harris, 1991, 1992). Structural field studies indicate that the Maubisse Nappe was overthrust only in places by the Banda Terrane, and in these places only by its thin southern edge (Harris, 1991). Perhaps the lack of thermal annealing experienced by the Maubisse Nappe is due to its distal location on the Australian continental margin, which preserved it from deep burial, and its structural position above the SDZ.

10. Rapid Late Neogene exhumation and cooling

The lack of unannealed fission tracks in apatite grains analyzed from Timor (fission tracks that formed at track-stable temperatures) can only be explained by recent and rapid exhumation and cooling from temperatures within the PAZ (60–120°C). The total amount of cooling is equal to the temperature of the PAZ, minus the mean annual surface temperature (20–30°C depending on elevation), which equals a possible range of cooling of 30–100°C. The time over which the cooling took place must be less than the time required to form new tracks, which is ~2 m.y. (Gleadow et al., 1983). Given a geotherm of 25°C/km this implies the removal of from 1.2 to 4 km of overburden during that time (0.6–2 mm/m.y.). Similar estimates are obtained from vitrinite reflectance values that are 0.6% *R*o higher (~90°C and 3.0–3.5 km of overburden) in rocks that were overthrust by the Banda Terrane.

Denudation rates for Timor based on paleobathymetry and chronostratigraphy of foraminifera found in the Central Basin of West Timor range from 3–10 mm/m.y., with the highest rates found near the RKA (de Smet et al., 1989). 40Ar/39Ar ages from the Aileu metamorphic complex (Berry and McDougall, 1986) yield denudation rates of around 3 mm/m.y. U/Th and 14C ages of Holocene coral terraces indicate surface uplift rates up to 1–3 mm/m.y. along the extension of the RKA in westernmost Timor and Roti (Vita-Finzi and Hidayat, 1991; Merritts et al., 1998).

These rates of exhumation far exceed those of thermal re-equilibration and those of apatite annealing. Even with low denudation at the slowest surface uplift rate estimates for Timor (0.3 mm/m.y.; Vita-Finzi and Hidayat, 1991), materials incorporated into the accretionary wedge would experience increased temperatures for a maximum of 1–2 m.y. Most annealing rate studies estimate a minimum of 2–5 m.y. is necessary to accomplish significant annealing in the PAZ (i.e. Gleadow et al., 1983). These observations have led us to mostly neglect the thermal affects of the Banda orogeny in interpreting variations of apatite fission track age in Timor. The only reasonable correlation we have found is between age variation and pre-collisional stratigraphic and structural position.

11. Time vs temperature relations

The pattern of paleotemperatures throughout Timor indicated by different methods is generally consistent in showing a northward increase in thermal maturity that is disrupted locally by faults (Fig. 5). This pattern correlates well south of the RKA and the Banda Terrane with the exposure of increasingly deeper stratigraphic and structural levels to the north. The Triassic to Pliocene units exposed in this region have a PPT that is similar and in some cases even lower than age equivalent units on the NW Australian shelf. There is no evidence that these units were thermally affected by the Banda orogen and therefore PPT must have been attained prior to accretion. Numerous oil and gas seeps throughout the southern Timor region attest to the low thermal maturity of that part of the accretionary wedge. This conclusion may also apply to Permian and Triassic units exposed in the RKA and the Maubisse Nappe.

In the Aileu Complex and some other units north of the RKA, an additional source of heat to that of stratigraphic burial is required to account for high *R*o values and metamorphism. Ar/Ar cooling ages of the north coast metamorphic assemblage indicate two thermal events of Neogene and >70 Ma age (Berry and McDougall, 1986). The Neogene age event is interpreted here as mostly a function of tectonic burial beneath the Banda Terrane and other parts of the orogenic wedge, both of which thicken to the north. Burial times of as much as 5–7 m.y. for the Aileu are also consistent with the zero fission track age obtained from the north coast metamorphic assemblage. However, in most other parts of the orogenic wedge the rates of accretion limit the duration of tectonic burial to the extent that its thermal affects are only partially recorded, if at all. Examples of this are local inconsistencies found between the maturation of vitrinite and apatite fission track annealing. *R*o values from the RKA of central Timor show peak temperatures of between 120 to 250°C, which is in the total annealing zone of apatite fission tracks. Yet, at the same location, apatite samples yielded old ages, which may be indicative of the different rates at which vitrinite and apatite thermally equilibrate.

Apatite FT modeling shows that maximum burial was during the Jurassic to ~90°C for the "older group" and hotter for the "younger". These temperatures were maintained with fluctuations until late Neogene, with perhaps some cooling. Rapid cooling from the PAZ occurred during the latest Miocene and Pliocene. This history with different temperature maxima can account for the variations in all samples.

12. Conclusions

The amount and distribution of heat during various stages of collision is commonly obscured in the rock record by later orogenic events and post orogenic thermal re-equilibration. This study demonstrates that in young orogens, where comparisons of pre- and post-accretion thermal conditions are possible, thermal effects are minimal for much of the material that moves through the orogenic wedge.

Indicators of PPT for Permian to Pliocene units accreted from parts of the NW Australian slope and rise show an increase in thermal maturity with depth that does not differ significantly from what is presently observed in unaccreted parts of NW Australia. Measurements of vitrinite reflectance, conodont alteration and illite crystallinity all show a general, but discontinuous increase in paleotemperature from south to north across the orogen, and an increase towards central Timor along orogenic strike. Many of the discontinuities correlate with faults. This pattern is consistent with the exposure of progressively deeper stratigraphic intervals towards the north and center of the island. Exposure to abnormally high paleotemperatures is indicated in the Aileu Complex, which experienced high heat flow during Jurassic rifting and Neogene arc–continent collision. The Neogene event was most likely a consequence of prolonged tectonic burial beneath the Banda Terrane forearc nappe in the hinterland of the orogen. Other units thrust beneath the Banda Terrane show a maximum of 90°C higher PPT than frontally accreted sequences.

Apatite FT age and track length distributions indicate that detrital grains with initial ages of approximately 300–400 m.y. were subjected to progressive heating due to burial at temperatures between 60–120°C until being exhumed during Pliocene collision-related shortening. These results also attest to the fact that little to no thermal overprinting accompanied the accretion process, and that PPT likely did not exceed that found at equivalent stratigraphic intervals drilled on the shelf. We attribute this to the fact that most of the accreted material in Timor resided on the slope and rise of the Australian passive margin and therefore experienced less long-term burial by thin overlying units.

Effects of the contractional accretionary event are manifest in the way apatite FT ages are inverted (younger over older) and the amount of variation over short distances. This relationship is interpreted as due to the combined effects of long-lived stratigraphic tapering of the Australian margin followed by rapid tectonic inversion. Inverted stratigraphic relations are best exposed in the core of the RKA, where deeper (more annealed) stratigraphic horizons are found at the highest elevations due to uplift associated with thrust emplacement and rapid exhumation. These mostly Permian to Lower Triassic sequences resided near the base of the apatite PAZ before cooling. Younger stratigraphic intervals are exposed at lower elevations with less total rock uplift. Cooling was recent and rapid enough to prevent any new tracks from accumulating, and to cause irregular responses of some paleotemperature indicators. These data preclude any accretionary event in the Timor region prior to the Late Miocene to Present arc–continent collision.

Acknowledgements

We wish to thank Union Texas Petroleum for supporting the bulk of the field and geochronological work associated with this study. Amoseas Indonesia, the National Science Foundation (EAR-9118151), and Western Mining Corporation of Australia provided additional support. The Geological Research and Development Center (GRDC) and University Pembangunan Nasional (UPN 'Veteran') sponsored Field studies in Timor. We thank Sahat Tobing, Carolus Prasetyadi and David Hunter for their contributions. John Renton assisted with clay mineralogy, Bill Grady provided vitrinite reflectance measurments and Walter Sweet analyzed conodonts. Paul O'Sullivan, Ann Blythe, Gomma Omar, Bart Kowallis, Tim Charlton, Tony Barber and Mike Audley-Charles contributed valuable reviews and discussion.

References

Abbott, M.J., Chamalaun, F.H., 1981. Geochronology of some Banda arc volcanics. In: Barber, A.J., Wiryosujono, S. (Eds.). Geology and Tectonics of Eastern Indonesia Special Publication of the Geological Research and Development Centre, 2 pp. 253–268.

Audley-Charles, M.G., 1968. The Geology of Portuguese Timor. Memoir of the Geological Society of London 4, 1–76.

Audley-Charles, M.G., 1983. Reconstruction of western Gondwanaland. Nature 306 (5938), 48–50.

Audley-Charles, M.G., 1986. Rates of Neogene and Quaternary tectonic movements in the southern Banda Arc based on micropaleontology. Journal of the Geological Society of London 143, 161–175.

Audley-Charles, M.G., 1988. Evolution of the southern margin of Tethys (north Australian region) from early Permian to late Cretaceous. In: Audley-Charles, M.G., Hallam, A. (Ed.). Gondwana and Tethys Geological Society of London Special Publication, 37 pp. 79–100.

Audley-Charles, M.G., Harris, R.A., 1990. Allochthonous terranes of the Southwest Pacific and Indonesia. Philosophical Transactions of the Royal Society of London 331, 571–587.

Barber, A.J., 1981. Structural interpretations of the island of Timor, eastern Indonesia. In: Barber, A.J., Wiryosujono, S. (Eds.). The Geology and Tectonics of Eastern Indonesia. Special Publication of the Geological Research and Development Centre, 2 pp. 183–197.

Barber, A.J., Audley-Charles, M.G., 1976. The significance of metamorphic rocks of Timor in the development of the Banda arc, eastern Indonesia. Tectonophysics 30, 119–128.

Barber, A.J., Audley-Charles, M.G., Carter, D.J., 1977. Thrust tectonics in Timor. Journal of the Geological Society of Australia 24, 51–62.

Berry, R.F., Grady, A.E., 1981. Deformation and metamorphism of the Aileu Formation, north coast, East Timor; its tectonic significance. Journal of Structural Geology 3, 143–167.

Berry, R.F., McDougall, I., 1986. Interpretations of 40Ar/39Ar dating evidence from the Aileu Formation, East Timor, Indonesia. Chemical Geology 59, 43–58.

Berry, R.F., Burrett, C., Banks, M., 1984. New Triassic fauna from East Timor and their tectonic significance. Geologica et Palaeontologica 18, 127–137.

Bird, P.R., Cook, S.E., 1991. Permo–Triassic successions of the Kekneno Group area, West Timor: implications for paleogeography and basin evolution. Journal of Southeast Asian Earth Sciences 6, 3/4, 359–371.

Bowin, C., Purdy, G.M., Johnston, C., Shor, G., Lawver, L., Hartono, H.M.S., Jezek, P., 1980. Arc-continent collision in Banda Sea region. American Association of Petroleum Geologists Bulletin 64, 868–915.

Breen, N.A., Silver, E.A., Hussong, D.M., 1986. Structural styles of an accretionary wedge south of the island of Sumba, Indonesia, revealed by Seamarc II side scan sonar. Geological Society of America Bulletin 64, 868–915.

Brown, M., Earle, M.M., 1983. Cordierite-bearing schists and gneisses from Timor, eastern Indonesia: P–T conditions of metamorphism and tectonic implications. Journal of Metamorphic Geology 1, 183–203.

Burham, A.K., Sweeney, J.J., 1989. A chemical kinetic model of vitrinite reflectance maturation. Geochimica et Cosmochimica Acta 53, 2649–2657.

Carter, D.J., Audley-Charles, M.G., Barber, A.J., 1976. Stratigraphical analysis of island arc–continental margin collision in eastern Indonesia. Journal of the Geological Society of London 132, 179–198.

Castano, J.R., Sparks, D.M., 1974. Interpretation of vitrinite reflectance measurement in sedimentary rocks and determination of burial history using vitrinite reflectance and authigenic minerals. Carbonaceous materials as indicators of metamorphism. Geological Society of America Special Paper 153, 31–52.

Chamalaun, F.H., Lockwood, K., White, A., 1976. The Bouguer gravity field and crustal structure of eastern Timor. Tectonophysics 30, 241–259.

Charlton, T.R., Barber, A.J., Barkham, S.T., 1991. The structural evolution of the Timor collision complex, eastern Indonesia. Journal of Structural Geology 13, 489–500.

Charlton, T.R., 1991. Postcollisional extension in arc-continent collision zones, eastern Indonesia. Geology 19, 28–31.

Charlton, T.R., 1992. Reply to Comment on 'Postcollisional extension in arc-continent collision zones, eastern Indonesia'. Geology 20, 92–93.

Crostella, A., 1977. Geosynclines and plate tectonics in Eastern Indonesia. American Association of Petroleum Geologists Bulletin 61, 2063–2081.

De Smet, M.E.M., Fortuin, A.R., Tjokrosapoetro, S., van Hinte, J.E., 1989. Late Cenozoic vertical movements of non-volcanic islands in the Banda arc area. Netherlands Journal of Sea Research: Proceedings of Snellius–II Symposium 24, 2/3, 263–275.

Dickinson, W.R., 1985. Interpreting provenance relations from detrital modes in sandstones. In: Zuffa, G.G. (Ed.), Provenance of Arenites, pp. 333–361.

Dropkin, M.J., Harris, R.A., Zeitler, P.K., 1993. An Oligocene forearc crustal flake exposed in a contemporary arc–continent collision: Timor, Indonesia. Geological Society of America Abstracts with Programs 25 (6), 482.

Epstein, A.G., Epstein, J.B., Harris, L.D., 1976. Conodont color alteration — an index to organic metamorphism. U.S. Geological Survey Professional Paper 995, 1–26.

Falvey, D.A., 1972. Sea-floor spreading in the Wharton Basin (northeast Indian Ocean) and the break-up of eastern Gondwanaland. Australian Petroleum Exploration Association Journal 12 (2), 86–88.

Fitzgerald, P.G., Gleadow, A.J.W., 1990. New approaches in fission track geochronology as a tectonic tool: examples from the Transantarctic Mountains. Nuclear Tracks and Radiation Measurements 17, 351–357.

Fitch, T.J., Hamilton, W., 1974. Reply to discussion on a paper by Fitch, T.J. Journal of Geophysical Research 79, 4982–4985.

Galbraith, R.F., 1990. The radial plot: Graphical display of spread of ages. Nuclear Tracks 17, 207–214.

Galbraith, R.F., Laslett, 1993. Statistical models for mixed fission track ages. Nuclear Tracks 21, 459–470.

Gallagher, K., 1995. Evolving temperature histories from apatite fission-track data. Earth and Planetary Science Letters 136, 421–435.

Gleadow, A.J.W., 1981. Fission track dating: What are the real alternatives? . Nuclear Tracks 5, 3–14.

Gleadow, A.J.W., Duddy, I.R., 1984. Fission track dating and thermal history analysis of apatites from wells in the north-west Canning Basin. In: Purcell, P.G. (Ed.), The Canning Basin, Geological Society of Australia Journal, pp. 377–387.

Gleadow, A.J.W., Duddy, I.R., Lovering, J.F., 1983. Fission track analysis: A new tool for the evolution of thermal histories and hydrocarbon potential. Australian Petroleum Exploration Association Journal 23, 93–102.

Gleadow, A.J.W., Duddy, I.R., Green, P.F., Hagarty, K.A., 1986a. Fission track lengths in the apatite annealing zone and the interpretation of mixed ages. Earth and Planetary Science Letters 78, 245–254.

Gleadow, A.J.W., Duddy, I.R., Green, P.F., Hagarty, K.A., 1986b. Confined fission track length in apatite: a diagnostic tool for ther-

mal history analysis. Contributions to Mineralogy and Petrology 94, 405–415.

Green, P.F., Duddy, I.R., Gleadow, A.J.W., Lovering, J.F., 1989. Apatite fission track analysis as a paleotemperature indicator for hydrocarbon exploration. In: Naeser, N.D., McCulloch, T.H. (Eds.), Thermal History of Sedimentary Basins: Methods and Case Histories. Springer-Verlag, New York, pp. 181–195.

Hamilton, W., 1979. Tectonics of the Indonesian region. US Geological Survey Professional Paper 1078, 1–345.

Hamilton, W., 1988. Plate tectonics and island arcs. Geological Society of America Bulletin 100, 1503–1527.

Harris, A.G., 1979. Conodont alteration, an organo-mineral metamorphic index, and its application to Appalachian Basin geology. In: Scholle, P.A., Schluger, P.R. (Eds.), Aspects of Diagenesis. Society of Economic Palaeontologists and Mineralogists Special Publication 26, pp. 3–16, Tulsa.

Harris, R.A., 1991. Temporal distribution of strain in the active Banda orogen: A reconciliation of rival hypothesis. Journal of Southeast Asian Earth Sciences 6 (3/4), 373–386.

Harris, R.A., 1992. Peri-collisional extension and the formation of Oman-type ophiolites in the Banda arc and Brooks Range. In: Parson, L.M., Murton, B.J., Browning, P. (Eds.). Ophiolites and their Modern Oceanic Analogues Geological Society of London Special Publication 60, pp. 301–325.

Harris, R.A., Sawyer, R.K., Audley-Charles, M.G., 1998. Collisional melange development: Geologic associations of active melange-forming processes with exhumed melange facies in the western Banda orogen, Indonesia. Tectonics 17, 458–480.

Helmers, J., Sopaheluwaken, J., Tjokrosapoetro, S., Surya, Nila E., 1989. High grade metamorphism related to peridotite emplacement near Atapupu, Timor, with reference to the Kaibobo peridotite on Seram, Indonesia. Netherlands Journal of Sea Research 24, 357–371.

Horstmann, E.L., 1989. Source maturity, overpressures and production, Northwest Shelf, Australia. In: Geology of the North West Shelf. Australian Petroleum Exploration Association, pp. 529–537.

Hurford, A.J., 1990. Standardization of fission track dating calibration: Recommendation by the Fission Track Working Group of the I.U.G.S. Subcommission on Geochronology. Chemical Geology 80, 171–178.

Hurford, A.J., Green, P.F., 1982. A users guide to fission track dating calibration. Earth Planetary Science Letters 59, 343–354.

Hurford, A.J., Green, P.F., 1983. The zeta age calibration of fission track dating. Isotope Geoscience 1, 285–317.

Karig, D.E., Barber, A.J., Charlton, T.R., Klemperer, S., Hussong, D.M., 1987. Nature and distribution of deformation across the Banda Arc–Australian collision zone at Timor. Geological Society of America Bulletin 98, 18–32.

Kenyon, C.S., 1974. Stratigraphy and sedimentology of the late Miocene to Quaternary deposits of Timor. Ph.D. dissertation, University of London, 290 pp.

Larson, R.L., 1975. Late Jurassic sea-floor spreading in the eastern Indian Ocean. Geology 3, 69–71.

Laslett, G.M., Green, P.F., Duddy, I.R., Gleadow, A.J.W., 1987. Thermal annealing of fission tracks in apatite 2: A quantitative analysis. Chemical Geology 65, 1–13.

Linthout, K., Helmers, H., Sopaheluwaken, J., 1997. Late Miocene obduction and microplate migration around the southern Banda Sea and the closure of the Indonesian Seaway. Tectonophysics 281, 17–30.

Marshallsea, S.J., 1991. Apatite fission track analysis of seven samples from Douglas - 1, Northwest Shelf, Geotrack report, 305, p. 35.

Merritts, D., Eby, R., Harris, R., Edwards, R.L., Cheng, Hai, 1998. Variable Rates of Late Quaternary Surface Uplift Along the Banda Arc–Australian Plate Collision Zone, Eastern Indonesia. In: Stewart, I.S., Vita-Finzi, C. (Eds.). Coastal Tectonics. Geological Society of London Special Publication 146, pp. 213–224.

Metcalfe, I., 1988. Origin and assembly of southeast Asian continental terranes. In: Audley-Charles, M.G., Hallam, A. (Eds.). Gondwana and Tethys Geological Society of London Special Publication 37, pp. 101–116.

Omar, G.I., Lutz, T.M., Giegengack, R., 1994. Apatite fission-track evidence for Laramide and post-Laramide uplift and anomalous thermal regime at the Beartooth overthrust, Montana–Wyoming. Geological Society of America Bulletin 106, 74–85.

O'Sullivan, P.B., Parrish, R.R., 1995. The importance of apatite composition and single-grain ages when interpreting fission track data from plutonic rocks: A case study from the Coast Ranges, British Columbia. Earth and Planetary Science Letters 132, 213–224.

Powell, D.E., 1976. The geological evolution of the continental margin off NW Australia. Australian Petroleum Exploration Association (APEA) Journal 16, 13–23.

Prasetyadi, C., Harris, R.A., 1996. Hinterland structure of the active Banda arc–continent collision, Indonesia: constraints from the Aileu Complex of East Timor. In: Proceedings of 25th Annual Convention of the Indonesian Association of Geologists, pp. 144–173.

Price, N.J., Audley-Charles, M.G., 1987. Tectonic collision processes after plate rupture. Tectonophysics 140, 121–129.

Reed, D.L., Silver, E.A., Prasetyo, H., Meyer, A.W., 1986. Deformation and sedimentation along a developing terrane suture: Eastern Sunda forearc, Indonesia. Geology 14, 977–1092.

Sani, K., Jacobson, M.L., Sigit, R., 1995. The thin-skinned thrust structures of Timor. In: Proceedings of the 24th Annual Convention of the Indonesian Petroleum Association, pp. 277–293.

Sawyer, R.K., Sani, K., Brown, S., 1993. The stratigraphy and sedimentology of West Timor, Indonesia. In: Proceedings of the 22nd Annual Convention of the Indonesian Petroleum Association, pp. 1–20.

Simons, A.L., 1940. Geological investigations in northeast Netherlands Timor. Geological Expedition of the Lesser Sunda Islands 1, 107–213. Amsterdam University.

Snyder, D.B., Prasetyo, H., Blundell, D.J., Pigram, C.J., Barber, A.J., Richardson, A., Tjokosaproetro, A., 1996. A dual doubly vergent orogen in the Banda Arc continent–arc collision zone as observed on deep seismic reflection profiles. Tectonics 15, 34–53.

Sopaheluwakan, J., Helmers, H., Tjokrosapetro, S., Surya, Nila E., 1989. Medium pressure metamorphism with inverted gradient associated with ophiolite nappe emplacement in Timor, Netherlands. Journal of Sea Research 24, 333–343.

Storey, B.C., Brown, R.W., Carter, A., Doubleday, P.A., Hurford, A.J., McDonald, D.I.M., Nell, P.A.R., 1996. Fission-track evidence for the thermotectonic evolution of a Mesozoic–Cenozoic fore-arc, Antarctica. Journal of the Geological Society of London 153, 65–82.

Veevers, J.J., Falvey, D.A., Hawkins, L.U., Ludwig, W.J., 1974. Seismic reflection measurement of northwest Australian margin and adjacent deeps. American Association of Petroleum Geologists Bulletin 58, 1731–1750.

Veevers, J.J., Cotterill, D., 1976. Western margin of Australia: A Mesozoic analog of the East African rift system. Geology 4, 713–717.

Vita-Finzi, C., Hidayat, S., 1991. Holocene uplift in West Timor. Journal of Southeast Asian Earth Sciences 6 (3/4), 387–393.

von der Borch, C.C., 1979. Continental-island arc collision in the Banda Arc. Tectonophysics 54, 169–193.

von Rad, U., Exon, N.F., 1983. Mesozoic–Cenozoic sedimentary and volcanic evolution of the starved passive continental margin off NW Australia. In: Watkins, J.S., Drake, C.L. (Eds.), Studies in Continental Margin Geology, American Association of Petroleum Geologists Memoir, 34, pp. 253–281.

Weiland, R.J., Cloos, M., 1996. Pliocene–Pleistocene asymmetric unroofing of the Irian fold belt, Irian Jaya, Indonesia; apatite fission-track thermochronology. Geological Society of America Bulletin 108, 1438–1449.